

9-30-1991

Bio-mechanics of the hip joint and the engineering considerations in the treatment of unstable intertrochanteric fractures

Manoj D. Nene
New Jersey Institute of Technology

Follow this and additional works at: <https://digitalcommons.njit.edu/theses>



Part of the [Biomedical Engineering and Bioengineering Commons](#)

Recommended Citation

Nene, Manoj D., "Bio-mechanics of the hip joint and the engineering considerations in the treatment of unstable intertrochanteric fractures" (1991). *Theses*. 2572.
<https://digitalcommons.njit.edu/theses/2572>

This Thesis is brought to you for free and open access by the Electronic Theses and Dissertations at Digital Commons @ NJIT. It has been accepted for inclusion in Theses by an authorized administrator of Digital Commons @ NJIT. For more information, please contact digitalcommons@njit.edu.

Copyright Warning & Restrictions

The copyright law of the United States (Title 17, United States Code) governs the making of photocopies or other reproductions of copyrighted material.

Under certain conditions specified in the law, libraries and archives are authorized to furnish a photocopy or other reproduction. One of these specified conditions is that the photocopy or reproduction is not to be “used for any purpose other than private study, scholarship, or research.” If a user makes a request for, or later uses, a photocopy or reproduction for purposes in excess of “fair use” that user may be liable for copyright infringement,

This institution reserves the right to refuse to accept a copying order if, in its judgment, fulfillment of the order would involve violation of copyright law.

Please Note: The author retains the copyright while the New Jersey Institute of Technology reserves the right to distribute this thesis or dissertation

Printing note: If you do not wish to print this page, then select “Pages from: first page # to: last page #” on the print dialog screen

The Van Houten library has removed some of the personal information and all signatures from the approval page and biographical sketches of theses and dissertations in order to protect the identity of NJIT graduates and faculty.

ABSTRACT

Title of Thesis: Bio-Mechanics of the Hip-Joint and the Engineering

Considerations in the Treatment of Unstable Intertrochanteric

Fractures

Manoj D. Nene, M. S. Engineering, October 1991

Thesis directed by: Dr. Raj S. Sodhi

Numerous previous attempts have been made to determine the magnitude and the direction of forces acting on the hip joint. The mechanism of femoral neck fractures and the frequently occurring failure of its internal fixation has led engineers to analyze the forces involved. An unstable intertrochanteric fracture is one which lacks continuity of the bone cortex on the opposing surfaces of the proximal and distal fragments. A mathematical model is created in this study to examine the 135° and 150° nail plate. The results give an approximate estimation of stresses on the two plates. A 3D finite element model of the two plates is created and the plate is loaded with different forces. Stress analysis of the two plates is performed to obtain the optimum design for an intertrochanteric fracture fixation device. A study is also made of the variables affecting the treatment of Unstable Intertrochanteric Fractures. This study concludes that the location of the plate and the plate angle affect the stresses as well as the treatment of the fractures. From the study we can conclude that the 150° plate is better than the 135° plate, since the stresses found in the 150° plate were calculated to be lower than the 135° plate.

1) **BIO-MECHANICS OF THE HIP JOINT AND THE ENGINEERING
CONSIDERATIONS IN THE TREATMENT
OF UNSTABLE INTERTROCHANTERIC FRACTURES**

by
1) Manoj D. Nene


**Thesis submitted to the faculty of the Graduate School of
The New Jersey Institute of Technology in partial fulfillment of
the requirements for the degree of
Master of Science in Engineering
1991**

APPROVAL SHEET

Title of Thesis: Bio-Mechanics of the Hip-Joint and the Engineering
considerations in the treatment of Unstable Intertrochanteric
fractures

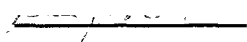
Name of Candidate: Manoj D. Nene
Master of Science, 1991

Thesis and abstract approved by:

 Dr. Raj Sodhi Date
Professor
Manufacturing Engineering
Dept.

Signature of other members
of the thesis committee

Dr. David Kristol Date
Director
Bio-Medical Engineering
Dept.

 _____
Dr. Rajesh Dave Date
Professor
Mechanical Engineering
Dept.

VITA

Name: Manoj D. Nene

Permanent Address:

Degree and date to be conferred: M. S., October 1991

Date of birth:

Place of birth:

Secondary Education:

Coll./Inst. attended	Dates	Degree	Date of Degree
M. S. Univ. of Baroda	06/79-04/84	B.S.M.E.	July 1984
Baroda, India			
N. J. I. T.	09/85-09/89	M. S.	October 1991
Newark, N. J.			

Major: Bio-Medical Engineering

Positions held: Research Assistant, 01/86-12/86

DEDICATION

I would like to dedicate this thesis to my parents and my family members whose support and encouragement helped me in furthering my education, and to my beloved wife who has been a constant companion and a source of inspiration through testing times.

ACKNOWLEDGEMENT

I would like to take this opportunity to thank my advisor Dr. Raj Sodhi for providing me with all the help and guidance necessary to successfully complete my thesis. I would also like to sincerely thank Mr. Katkuri Reddy, M. E. Dept. for spending his invaluable time in assisting on the CAD portion of the thesis work. Last but not the least I would like to thank Dr. David Kristol, Chairman of the Bio-Medical Engineering program for his patience and help in completing the Masters program.

TABLE OF CONTENTS

I. Introduction

1.1 Background	1
1.2 History	1
1.3 Definition of Intertrochanteric Fracture	7
1.4 Materials of Construction/Implant Material	8
1.5 Previous Fixation Methods/Techniques	9
1.6 Modern Techniques	11
1.7 Previous Finite Element Studies	12
1.8 Objective of Present Study	18

II. Mechanics/Stress Analysis of Intertrochanteric Fracture

2.1 Mechanics of Intertrochanteric Fracture	20
2.2 Mechanics of Sliding Fixation Devices	20
2.3 Mathematical Analysis of Stress in the Human Femur	30

III. Biomechanics and forces acting on the hip-joint

3.1 Bio-Mechanics of the Hip	33
3.2 Forces acting on the Hip Joint	33

IV. System Model	39
------------------------	----

V. Computer Aided Design and Finite Element Modeling	46
5.1 Definition of I-DEAS	46
5.2 Solid Modeling	47
5.3 Engineering Analysis	47
5.4 System Dynamics	49
5.5 Test Data Analysis	49
5.6 I-DEAS	50
5.7 Solid Modeling	50
5.8 Engineering Analysis	51
5.9 System Dynamics	52
5.10 Test Data Analysis	52
5.11 Methodology	52
5.12 2-D CAD Software	56
5.13 3-D CAD Software	58
5.14 Hardware support for 2-D and 3-D software	59
5.15 Analysis Software	61
5.15.1 Capabilities of a FEA Software	61
5.15.2 General Structure of a FEA Software	62
VI. Conclusions	65
VII. Bibliography	71

LIST OF TABLES

I. Comparative study of failures in various plates	77
II. Proportion of elements in S. S. nails used for Orthopaedic implants	82
III. Muscle and joint forces calculated at various positions of walking cycle ...	83

LIST OF FIGURES

1. Hip-Joint: A Ball and Socket Joint	2
2. Geometrical skeleton of the femur illustrating functional axes, applied angles and planes	4
3. Definition of Intertrochanteric Fracture-4 Sections	6
4. Method of Guide Pin Placement	10
5. Element Mesh of the Human Femur	13
6. Resultant Force-Parallel and Perpendicular Components	22
7. Free Body Diagram of a Compression Hip Screw	24
8. Force Applied to Initiate Sliding	28
9. Force Diagram of the Normal Femur	34
10. Beam Analysis of the Plate	38
11. Solid Model of a 135° plate	53
12. Solid Model of a 150° plate	54
13. Classification of screw position in the femoral head	64
14. Plot of σ_x v/s 'X' for 135 ° plate	69
15. Plot of σ_x v/s 'X' for 150 ° plate	70

CHAPTER I

INTRODUCTION

1.1 Background:

Internal fixation of intertrochanteric hip fractures with a sliding hip screw or nail has proven to be a superior method of fixation as compared to the use of rigid nail-plate devices.

The sliding device allows controlled impaction of bone fragments to a stable configuration, restoring the medial weight-bearing buttress of bone. This allows load transmission across the fracture site and makes early ambulation with full weight bearing possible. The sliding action also minimizes the possibility of nail penetration and cut out.

1.2 History:

Galilei along with others like Ward⁴², Wyman⁴⁶, Haughton¹⁹, Pauwels have all discussed the load bearing capacity of bones. They all felt that there is a relation between the design and function of the bone. The design of the proximal femur, the head and the neck, and it's internal architecture has been the subject for mechanical analyses. The femoral head is not exactly spherical in shape but, slightly compressed in an approximately ventro-dorsal direction. The femur is both non-linear and non-homogenous in geometry. The femur has both a mixture

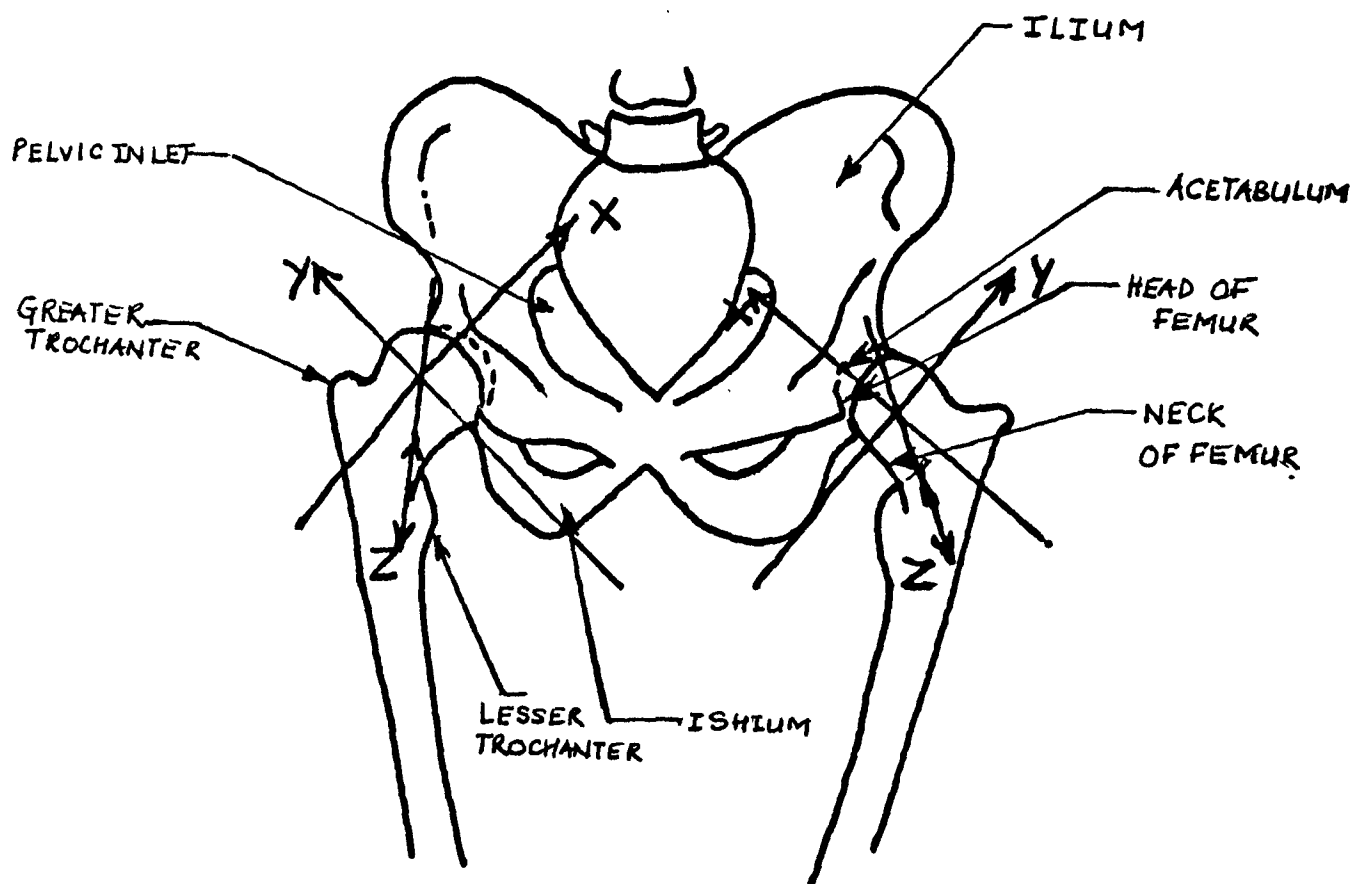


Fig. 1 Hip-Joint: A Ball and Socket Joint

of isotropic and anisotropic properties. The femoral neck lies in a distal-lateral direction. It is like a long tube compressed in the ventro-dorsal direction. The neck changes shape during its entire length. A section through the neck is almost cylindrical at its junction with the head. The shape of the neck becomes elliptical in a distal lateral direction.

The cortical shell of the neck is as thin as paper at its head. As the shaft is approached the cortical bone increases its thickness gradually. In the superior part of the neck, the increase is small, but in the inferior part, the thickness increases considerably and is maximum where the major axis intersects the cortical bone. Hence, in a section through the major axis the cortical bone is strongest in the inferior part.

The hip-joint is a ball and socket type of joint composed of acetabulum and the femoral head as shown in Figure 1. The cartilage covering the femoral head has non-uniform thickness, which results in different elastic properties in different regions of the femoral head. These different mechanical properties from point to point affect the transmission of stresses from the acetabulum through the femoral head to the femoral neck. The distribution of stresses on the femoral head is very complex.

To understand the design of the upper femur and its relationships to the forces acting on the bone, the angle formed by the neck with the femoral shaft must be known.

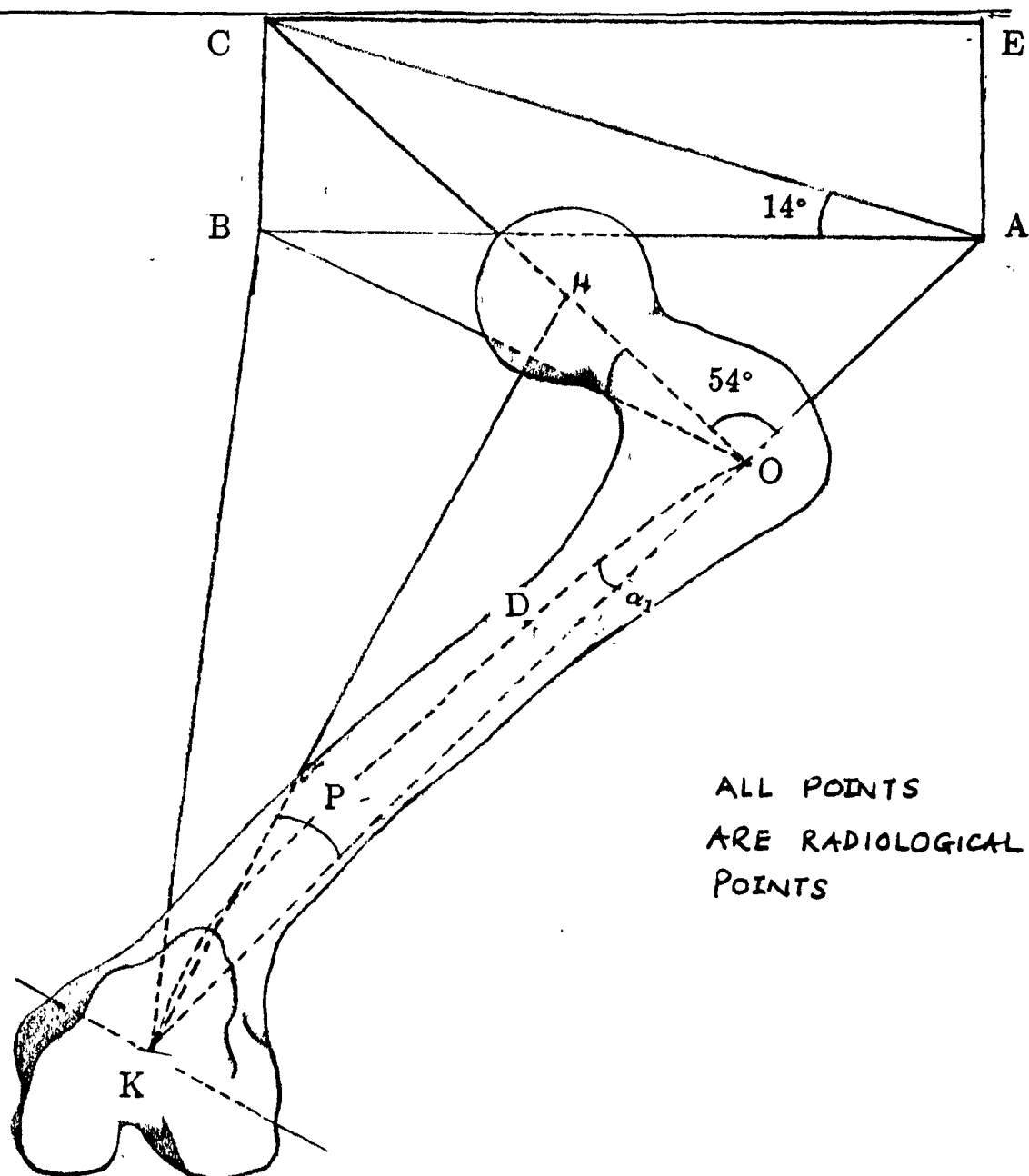


Fig.2 Geometrical skeleton of the femur illustrating functional axes, applied angles and planes.

The angle formed by the neck of the femur and the shaft, the cervico-diaphyseal angle is defined as the angle formed between the cervical axis OHC and the ideal axis AOK (Fig.2). On an average this angle is about 54° .

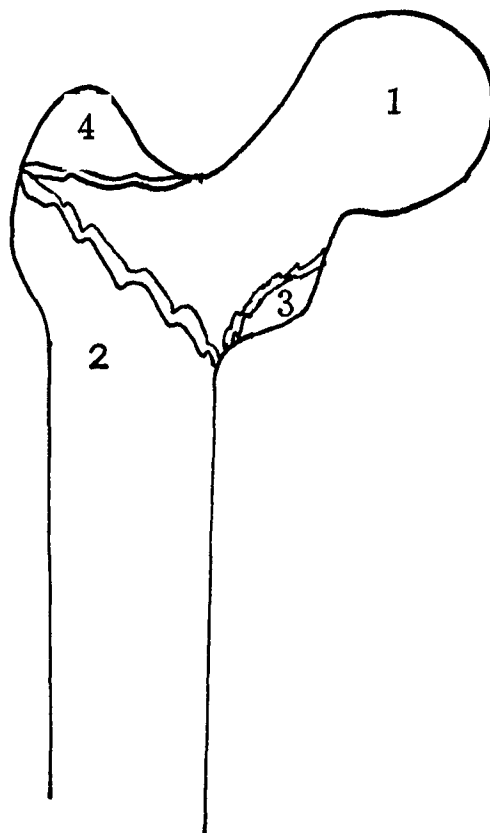
The cervico-diaphyseal angle can also be defined as the angle formed by the cervical axis OHC and the proximal longitudinal axis of the femoral shaft OD.

A plane through the ideal axis and the cervical axis AOKC is called the antetorsion or the anteversion plane (Fig. 2). The mobility in the hip-joint and the force relationships are functions of the cervico-diaphyseal and ante-torsion angles.

The variations of the cervico-diaphyseal angle, the antetorsion angle and the principal plane under normal and pathological conditions have been the subject of different mechanical interpretations. Investigators in this field feel that changes can take place in the design of the bone in order to permit yielding to existing mechanical stresses.

Milch²⁸ maintained that the direction of the resulting force can be determined by the analysis of the internal structure. Gluckmann¹⁷ believed that the tensile stress provokes the formation of bone and affects the architecture. Pauwels on the basis of theoretical analysis and experiments believed that the trabecular system is built up in order to achieve a framework with minimum of material.

Bone apposition and resorption are caused by the magnitude of stress and due to remodeling, the lamellae will have the same direction as though they were stress lines. Stress on the epiphyseal cartilage according to Pauwels may affect the



- 1- HEAD OF FEMUR
- 2- NECK OF FEMUR
- 3- LESSER TROCHANTER
- 4- GREATER TROCHANTER

Fig. 3 Intertrochanteric Fracture- Four Sections

bone growth. Tensile stress on the epiphyseal cartilage would simulate growth in length, while thickness is determined by compressive stress.

Kummer felt that the skeleton is built up with a minimum of material in order to resist the required stress. The upper femur can be regarded as a crane, but he disapproved photo-elastic tests on the models for analysis of the trabecular system, as the magnitude and direction of forces acting on the hip joint are unknown.

Symth³⁹ inquired about a quantitative method for measuring forces in the hip-joint, as the muscular force is difficult to evaluate. He believed that bones can be formed to resist stress in the best possible way. Garden¹⁵ believed that the internal architecture of the femur cannot be determined by mechanical principles, but that the structure arises through rotation and expansion from the shaft of the femur.

1.3 Definition of Intertrochanteric Fracture

An unstable intertrochanteric fracture of the femur is shown in Fig. 3. An unstable intertrochanteric fracture lacks continuity of the bone cortex, on the opposing surfaces of the proximal and distal fragments. This cortical defect is due to either comminution on the medial aspect of the neck (calcar region), or a large and separate posterior trochanteric fragment. Sometimes combination of the two is present. The instability is generally unrecognized, and anatomical reduction does not restore stability.

The internal fixation of intertrochanteric hip fractures with a sliding hip screw or a nail has proven to be a superior method of fixation. The sliding device allows a more uniform load distribution at the fracture site, which makes early ambulation and full weight bearing possible.

1.4 Materials of Construction of Sliding Devices

Failures of many of these nails initiated study of design and the construction of a nail, which could be trusted to withstand the stresses, normally encountered in the post-operative period, of the typical elderly patient, with an intertrochanteric fracture.

Secondary consideration in the design of a stronger nail plate was the possibility, that many elderly patients would safely be encouraged to bear weight on the fractured hip, thereby acquiring the obvious advantages of bi-pedal gait. In intertrochanteric fractures however, the problem is more complex because of osteoporosis, comminution and the consequent difficulty in securing truly strong fixation.

From Table I, it can be seen that various types of nails such as Smith-Petersen, McLaughlin, Jewett type, Holt, V-nail plate were used for analyses. The metals that were primarily used were S.S. 301, S.S. 316, A-286, AISI 316, CoCr alloys, SMO S.S., Titanium and Vitallium. The angle of the nails used varied from 125° to 155°. The maximum load bearing capacity was found to be in a Holt-Vitallium 130° type of nail which was angle mounted at 3/4" above the edge of

the plate. Most of these nails were mounted either 1/2", 3/4" , 7/8", 1" or 1 1/8" above the mount. The common failure among these nails was found to be plate bending at the top screw hole, at the nail plate junction or at the mount.

1.5 Previous Fixation Methods/Techniques

Functional recovery can be achieved by both operative and non-operative treatment of intertrochanteric fractures. The operative treatment is preferred because, following adequate internal fixation of these fractures, the patient is spared the hazards and expense of prolonged recumbency.

There have been various suggestions by authors concerning the treatment of comminuted unstable intertrochanteric fractures. Evans¹¹ advocated fixation in the position of varus deformity, while Dimon and Hughston¹⁰ advised medial displacement of the distal fragment. Boyd and Anderson¹ suggested placing a buttress plate laterally to prevent varus displacement, but accepted that medial displacement of the distal fragment, at the time of the operation is often the only way of achieving stability, in these comminuted unstable fractures. All authors have emphasized the importance of creating bony stability at operation.

Stable intertrochanteric fractures are satisfactorily treated with rigid internal fixation devices, but recognition of the type of fracture which will be satisfactorily stabilized is not always possible as pre-operative radiographs do not reveal the extent of comminution that is present.

Surgeons use guide pins⁹ to help insert the nail. Using the guide pin helps

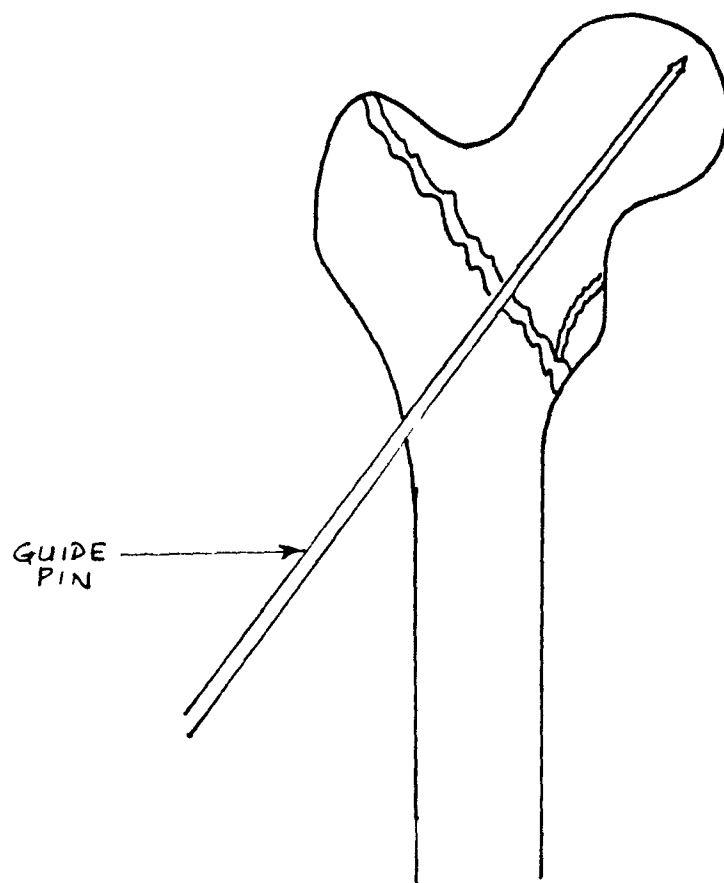


Fig. 4 Method of Guide Pin Placement

in ensuring proper placement of the screw and prevents destruction of bone because of repeated insertions. The guide pin also establishes the exact length of the nail and permits placing the nail at the same angle to the shaft, as the fixed angle of the nail plate.

Treatment of intertrochanteric femoral fractures is achieved through the use of Sliding Screw Plates, while treatment of trochanteric fractures is achieved using Compression Screws, Nail plates.

1.6 Modern Fixation Devices

In recent years the development of the hip fixation devices has led manufacturers to use superior quality materials, to produce nails and sliding devices. Materials like Vitallium, alloys of Titanium, Molybdenum, Chromium, are used which have strong mechanical properties and are easy to manufacture.

Dow Corning utilizes 316 LVM S. S. ASTM F-55 as its material of construction for all its fixation devices. DePuy uses its own DePuy certified S. S. as its material of construction. The sizes for tube length for both the 135° and the 150° compression screw manufactured by Dow Corning varies from 38 mm to 64 mm, while the plate length varies from 102 mm to 152 mm for the Dow screw. The Synthes screw has two tube lengths, 25mm and 38mm, while the plate length varies from 46mm to 270mm. Similarly in case of DePuy the plate length comes in varying sizes from 70 to 260mm for the compression hip screw. The number of holes vary from 2 to 12 for the three screws.

The nail length for a 135° or 150° Jewett nail manufactured by DePuy varies from 50 mm to 305mm, while the plate length varies from 89 mm to 146mm. The number of holes vary from 3 to 6.

1.7 Previous Finite Element Studies

The Finite Element Method(FEM) is an advanced computer technique of structural stress analysis developed in Engineering Mechanics, introduced to Orthopedic Bio-Mechanics to evaluate stresses in human bones. Since then, this method has been applied for stress analysis of bones, bone-prosthesis structures, fracture fixation devices and various kinds of tissues other than bones.

FEM analyses are based on theories of continuum mechanics. The continuum materials involved in the analysis of bones are the cortical (or compact) bone, and the trabecular (or spongy) bone. On a macroscopic level the trabecular bone is noncontinuous, and hence considered a structure rather than a material. But, in quasi-static loading, both cortical and trabecular bone behave linear elastic by approximation (although they are considered anisotropic and non-homogeneous). Their elastic properties depend on age, species and mineral content.

The cortical shafts of the long bones, have irregular beam-like geometries. Their metaphysical and epiphyseal ends are irregular in shape. Bone loading is dynamic due to muscle and gravitational forces, and little is known about its characteristics.

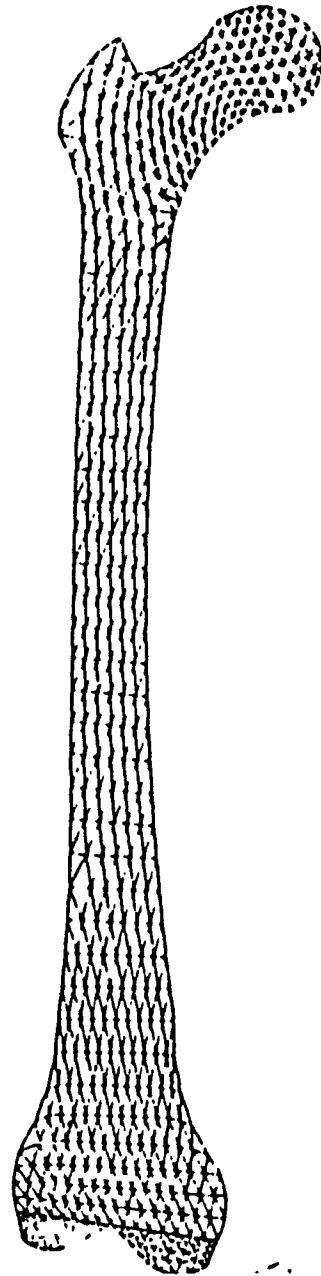


Fig. 5 Element Mesh of the Human Femur

Finite element analysis is presently being used to investigate the stress-related architecture of bone, and bone remodeling processes, to test and to optimize, artificial joint designs and fracture fixation devices, and to study the mechanical behavior of tissues, such as articular cartilage and intervertebral discs.

The femur is the most frequently analyzed bone due to its involvement in orthopedic treatments, such as prosthetic replacement of fracture fixation. Early FEM for stress analysis of the femur by Brekelmans² (fig. 5) and Rybicki³⁶ were aimed at demonstrating the possibilities of the FEM. They both applied 2-D plane stress elements of uniform thickness, by varying the Young's moduli of the elements. Rybicki only analysed the proximal part of the bone, accounting for non-uniform thickness. The results were comparable to a 2-D beam model analysis, but only agreeable in the diaphyseal part. A similar model was used by Wood⁴⁵ et al.

The early 3-D FEM models of the femur demonstrated the problems associated with data manipulation, interpretation and representation. Some models contained a high degree of sophistication, such as realistic non-homogeneity of trabecular bone. The data generated for the shaft of the femur, compared favorably among different mathematical models.

The 3-D model developed by Scholten is a refined one, with a high mesh density (approximately 10,000 degrees of freedom). Valliappan's⁴⁵ model consisted of higher order elements. Valliappan et al. roughly compared FEM results with those of stress-coat experiments, revealing good agreement in a relative sense.

Rohlmann³⁴ et al. achieved the same conclusion, based on a comparison between 3-D FEM and strain-gage experimental results, from paired femoral bones.

Huiskes et al.²³ showed through detailed experimental and theoretical analyses on bilateral bones, that the femoral shaft can be modeled refined, when the cortical bone is assumed to be transversely isotropic.

A 2-D Finite element model of the femoral head was developed by Brown and Ferguson³. It included nonhomogeneous elastic properties of trabecular bone. The study was aimed at investigating the influences of trabecular bone nonhomogeneity and of geometrical varus-valgus alterations on the stress distribution. Brown et al.⁴, later extended the model to the proximal femur, where anisotropy was included and mechanics of the femoral head in presence of avascular necrosis were studied.

Brown et al.⁵, developed a 2-D FEM model of the proximal femur, to study the collapse phenomenon of trabecular bone in aseptic necrosis including non-linear elasto-plastic material behavior.

Similarly other researchers subjected their studies towards bone growth and remodeling. Hayes²⁰ et al., attempted to correlate the trabecular bone architecture of the human patella, and its stress distribution for the quantification of Wolff's hypothesis. They found that high Von Mises effective stress, correlates with regions of high trabecular density, and that the trabecular structure aligns itself with principal stress orientations. They also demonstrated that anisotropy

of trabecular bone hardly affects the stress distribution, if its nonhomogeneity is accounted for.

Pugh³² et al., studied stresses in the trabeculae using simple plate elements. The aim was to correlate local bone loading with trabecular failure. A 2-D FEM model was proposed by Williams and Lewis⁴³, to predict the elastic constants of trabecular bone as a continuum material, from the non-continuous trabecular structure and properties.

Stress related remodeling of bone, investigated by Hassler et al.¹⁸, evaluated stress predictions in a piece of rabbit skull, loaded locally by an apparatus applying 2D and 3D models. The stress distribution was evaluated at particular time intervals.

Chand et al.⁷, used a 2-D FEM model and an iterative algorithm to investigate the unbonded elastic contact problem between femur and tibia in the knee joint. Results were comparable to those of 2-D and 3-D photoelastic analyses. A simpler 2-D model of both the tibia-femoral, and the femur-patellar complex was reported by Valenta et al.⁴⁰, in which contact areas were presumed. Hayes et al.²⁰, presented an axisymmetric FEM analyses (non-axisymmetric loading) of the upper tibia. Hayes was effective in demonstrating the load transmission in the upper tibia and its relation to the bone structure.

A 3-D FEM model of the lower femur and upper tibia was reported by Roehrle et al.³³, Roehrle did not model the whole tibia. Piziali³⁰ et al., used the FEM to

solve Saint Venant's warping function for torsion, in a cross-section of this bone.

Fracture Fixation Devices:

In recent years interest has been focussed on the fracture fixation devices, because the use of fracture fixation devices may weaken the bone through disuse osteoporosis or bone resorption, particularly due to the application of bone screws and pins. There have been suggestions that bone-remodeling and bone-resorption phenomenon may be initiated by micro-fractures, which would be of importance in implant design and fixation. Fracture mechanics of the bone have not been studied with the FEM, although considerable advances in this area were reported for other materials in engineering mechanics.

The fracture fixation devices are used extensively in orthopedic and general surgery. Their mechanical characteristics are important due to strength requirements, and the influence of their fixation rigidity on the fracture healing process. Use of the FEM in an analysis of a bone-fracture plate complex was first reported by Rybicki³⁵ et al. Subsequently Rybicki and Simonen³⁶ analysed a 2-D FEM model, of an oblique fracture stabilized with bone plates. Stresses at the fracture site were evaluated, for varying circumstances, such as pretension in plate, bone screw orientation and bone loading.

Simon et al.³⁸, performed an extensive comparison of beam, 2-D and 3-D FEM models, and experimental findings with respect to the bone plate. All three models gave comparable results, but more detailed information was obtained from

from the 3-D model at a specific location. The FEM beam model in the study was subsequently studied by Woo et al.⁵⁰, to study bone remodeling, comparing FEM results to the remodeling findings in animal experiments. Carter⁶ et al., studied bone remodeling in particular by comparing stress fields, with in-vivo bone resorption phenomena. The FEM was applied for local cross-section, to evaluate shear-stresses in torsional loading.

Using 3-D FEM beam elements Chao and An⁸, evaluated frame rigidity in several configurations out of different materials, in combination with experimental analyses. The sites, at which the pins of these frames are connected to bone are usually heavily stressed, making bone liable to pressure necrosis.

Fracture fixation by nailing received attention where FEM analysis was concerned. A 3-D non-linear FEM model to study trochanteric femoral fractures was presented by Ghassemi¹⁷ et al. Valenta⁴⁴ et al., previously studied a linear 2-D FEM model. Due to the large variety of fracture types, it is doubtful whether an anatomic (geometrically refined) 3-D model is helpful in analyzing these structures, especially when non-linear effects are taken into account. Hence, it would be realistic to aim for general information on a relative basis, in the case of fracture fixation FEM modeling.

1.8 OBJECTIVE:

This work examines the variables involved, in the treatment of unstable intertrochanteric fractures of the hip. The study will identify the variables involved

in the placement of the lag screw, and in the design of the screw plate. The study shall also investigate the biomechanics of the hip joint to determine the transmission of forces through the femoral neck, identifying the variables involved like the plate angle, and the eccentricity of the screw-plate. A mathematical model is developed to obtain the relationships between these variables, and study the possibility of theoretically determining the optimal design, of the screw positioning and the plate geometry. A 3 -dimensional finite element model of the plate is also developed to study the stresses developed, and a comparison of stresses acting on the plates is done to determine an optimal design. Design modifications are suggested to alleviate the stresses at the corners of the plates.

CHAPTER II

Mechanics/Stress Analysis of Intertrochanteric Fracture:

2.1 Mechanics of Intertrochanteric Fracture

Proper use of a sliding screw or nail requires an understanding of the mechanics of the intertrochanteric fracture as well as the mechanics of the device used. The stability of the proximal femur depends primarily on the medial cortex. When a significant segment of the medial cortex is fractured, as in an unstable intertrochanteric fracture, the stability is lost, which allows the fracture to displace into varus. The integrity of the medial weight-bearing buttress of bone must be restored, before ambulation with full weight bearing is possible. The medial buttress can be reconstituted with osteotomies, or medial displacement, or by allowing impaction of fracture fragments so that this area resumes its function as a load-carrying structure. If this is not done and the patient is allowed to ambulate, the forces generated across the hip are so great that nail penetration, breakage, cut out and various deformities may occur.

2.2 Mechanics of Sliding Fixation Devices

The use of compression hip screws for the internal fixation of hip fractures has gained popularity in recent years, because of its ability to provide solid

bending fixation of the two major fracture fragments, while allowing physiological compression at the fracture site and minimizing the possibility of nail penetration or cut-out. The controversy over the use of a high or low angle plate in the placement of the screw remains unsolved. It is advantageous to have a low-angle nail because of its ease of insertion. Massie and others have asserted that as the angle of the nail plate approaches the normal weight-bearing axis of the hip, the bending moment on the nail decreases. This may result in greater ease of sliding of a compression hip screw, less potential for jamming, and better bone impaction at the fracture site.

To understand the mechanics of a sliding fixation device, one must first understand the forces that act on the device. The magnitude and direction of the force exerted across the hip joint are dictated by the body weight, and the muscles acting on the hip.

In 1935, Pauwels published studies on the forces about the hip applied at an angle of 60° to the horizontal plane, and concluded that they represent about three times the body weight, in a single-leg stance phase. These results were confirmed by others. Frankel¹² showed that after osteosynthesis of experimentally created femoral-neck fractures, the bone absorbs as much as 75 percent of the load applied to the femoral head. Applied load on the nail plate can therefore be assumed to be 25 percent of the resultant load, during single-leg stance phase for an average adult person. This load represents the minimum force applied to the

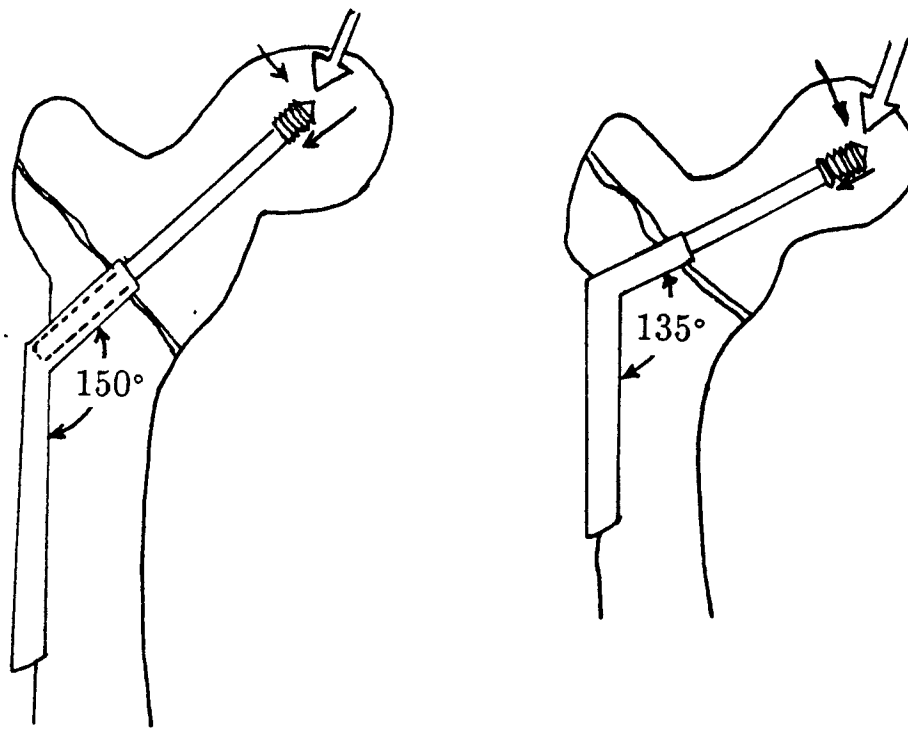


Fig. 6 Resultant force divided into two components, parallel and the other perpendicular to the sliding axis of the screw.

screw in a patient who would be allowed to walk immediately after osteosynthesis.

The resultant force (Fig. 6) across the hip can be resolved further into components parallel and perpendicular to the screw axis. Only the perpendicular component creates a bending moment in the screw. The magnitude of the perpendicular force component applied to the screw is dependent on the divergence of the screw plate angle from the normal weight-bearing axis of the hip.

As the angle of the sliding axis of the fixation device neared the direction of the resultant force acting on the hip, the greater was the force exerted to slide the device. As the nail-plate angle of the fixation device digressed, from the direction of the resultant force acting on the hip, a weaker force was exerted parallel to the sliding axis. A large perpendicular force was undesirable, since it would act to bind or jam the sliding mechanism preventing fracture impaction.

To calculate the perpendicular load on the screw, we consider a 2000-newton force acting on the hip joint weighing 154 lbs., in the single-leg stance phase of gait. Since Frankel¹² concluded that bone absorbs 75 percent of this load in the presence of a fracture-fixation device. The minimum force that will be exerted on the screw is 500 newtons (25 percent of 2000 newtons). When resolved into components parallel and perpendicular to the screw, the resultant perpendicular to the screw, the resultant perpendicular load component for a 130° nail plate is equal to

$$B_0 = 500 \sin[159 - 130]^\circ = 242.4 \text{ newtons}$$

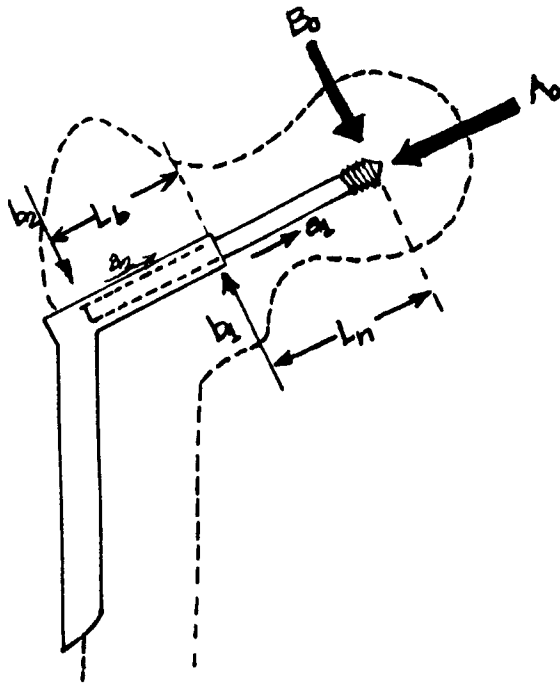


Fig. 7 Free Body Diagram of a Compression Hip Screw showing resultant force applied across the hip divided into perpendicular load(B_o)and an axial load (A_o); b_1 , b_2 -perpendicular reaction forces and a_1 , a_2 -resultant frictional forces.

Similarly the resultant perpendicular load component for a 150° nail plate is equal to

$$B_0 = 500 \sin[159 - 150]^\circ = 78.22 \text{ newtons}$$

The force component parallel to the barrel was the component that produced sliding of the screw. When the parallel component exceeded the maximum static frictional force between the screw and the barrel, sliding was initiated. This maximum static frictional force was controlled by the magnitude of the perpendicular force component, and the actual coefficient of friction between the sliding surfaces.

Fig. 7 shows a free-body diagram. The force B_0 acting perpendicular to the screw applied over the distance L_n must be counteracted by the reaction forces b_1, b_2 created between the screw shaft and the barrel acting over the distance L_b . Since the distance L_b was shorter than the distance L_n , the reaction forces created at the screw barrel interface were great. The parallel force A_0 acting to slide the screw was counteracted by the frictional force between the screw shaft and the barrel a_1, a_2 as a result of the perpendicular load B_0 .

As the nail-plate angle increased the ease of sliding increased in an exponential manner. Clinically, no control exists over the length of the screw extending from the barrel (L_n), because the screw must be placed well into the femoral head to obtain maximum purchase of the proximal fragment. The amount that the screw is engaged in the barrel would then be controlled.

The sliding characteristics of any of these devices are determined by two parameters: the apparent coefficient of friction and the actual coefficient of friction. The actual coefficient of friction is simply defined as the ratio of the amount of force required to slide pieces of metal one over the other (force parallel to the surfaces) to the amount of force pushing over the two surfaces together (force perpendicular to the surfaces). This coefficient of friction is usually thought to be dependent on the material and the nature of the surfaces of those materials.

The apparent coefficient of friction is a property not only of the type of material and the surface finish but also of the geometric characteristics of the sliding hip nail. The apparent coefficient of friction is defined as the ratio of the force parallel to the screw barrel (A_o) that is required to initiate sliding when the tip of the screw is loaded with a force applied perpendicular to the barrel (B_o). Here, the amount of force required to initiate sliding will depend on the length of the screw extending from the barrel (L_n) as well as the length of the screw in contact within the barrel (L_b).

From the conditions of static equilibrium and the assumption that the actual coefficient of friction (μ) is defined as the ratio of the tangential forces (a_1 and a_2) to the normal forces (b_1 and b_2) at the contact points between the screw and barrel, the following expression for μ is obtained:

$$\mu = \frac{a_1}{b_1} = \frac{a_2}{b_2} \quad (2.1)$$

$$\mu = \frac{A_o/B_o}{1 + 2\frac{L_n}{L_b}} \quad (2.2)$$

Therefore, the actual coefficient of friction between the sliding surfaces (μ) is determined from the earlier equation while the apparent coefficient of friction (μ_o) is determined from its definition

$$\mu_o = \frac{A_o}{B_o} \quad (2.3)$$

where A_o is the parallel load component and B_o is the perpendicular load component at the proximal tip of the screw.

Tests have been carried out by previous researchers to examine the effect of screw-plate angle on the sliding characteristics and jamming potential of four commonly used S.S. and CoCrMo compression hip screws. The actual coefficient of sliding friction for these alloys was also measured in each device. The force on the screw required to overcome the static frictional force was also determined, representing 130-degree and 150-degree screw-plate angles. For the 130-degree plate this force was significantly higher²⁹ than that required for the 150-degree loading configuration. The actual coefficient of friction was found to be relatively constant for each material.

If the length of the screw extending from the barrel is very long as compared to the length engaged in the barrel, jamming occurs. Jamming results from gross surface distortion in an uneven and unpredictable manner between the two

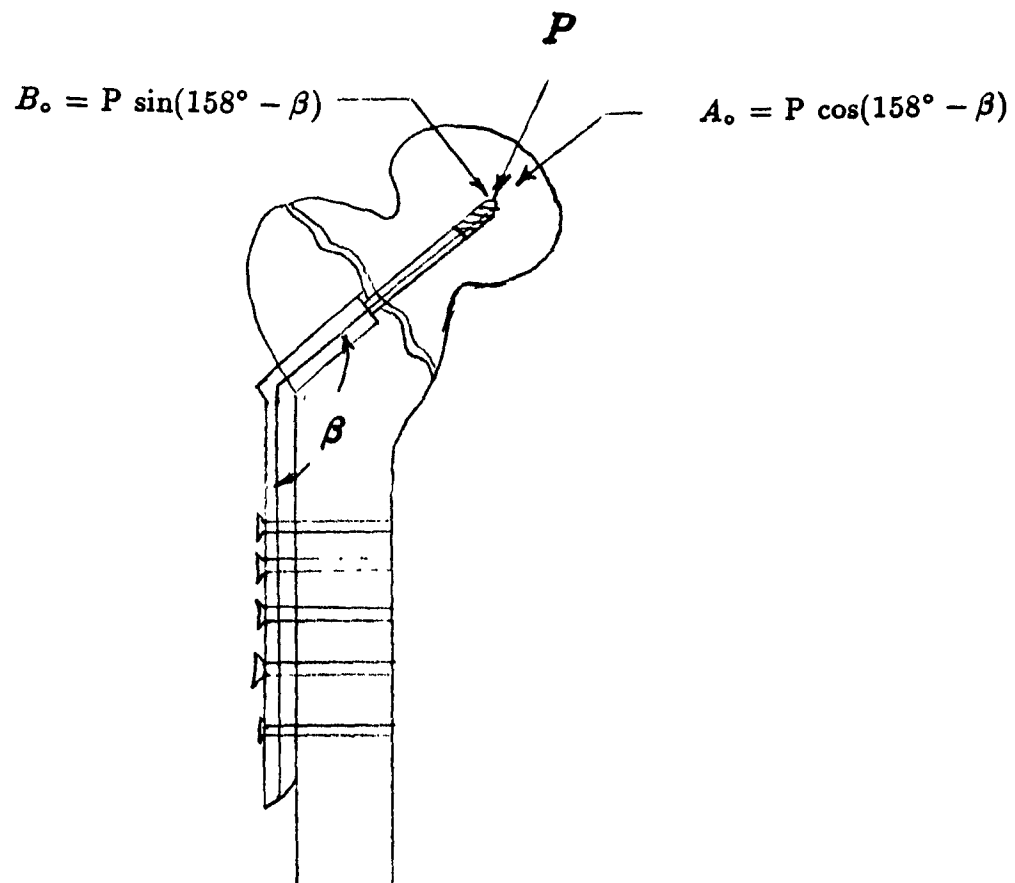


Fig. 8 Load applied to initiate sliding

surfaces, and this distortion greatly increases the actual coefficient of friction, and prevents surface sliding. The composition of metal alloy also influences jamming.

Results²⁹ have shown that all 316L S.S. screws jammed when tested at the 130-degree loading configuration, with the screw extending 10.2cms from the end of the barrel. It was also found that none of the screws jammed at the 150-degree loading configuration. The maximum static frictional force that was required to initiate sliding for the 130-degree loading configuration was significantly higher than that measured for the 150-degree loading configuration.

From these tests²⁹ it was clear that two factors appear to control the ease of sliding and the potential for jamming. The first was the amount of contact force generated between the distal tip of the screw, and its surface of engagement within the barrel. As the screw was extended from the barrel, the contact forces within the barrel increases. The second factor influencing the potential for jamming is the composition of the metal alloy.

In an intertrochanteric fracture the choice of the screw angle (β) was an important consideration. In order for sliding to occur, the parallel load component (A_o) applied to the tip of the screw must exceed the load (A) required to initiate sliding. So, the ratio A_o/A was a measure of the sliding capability of the device.

In Fig. 8 a load P was applied to the tip of the screw. Assuming this load to be directed at 158 degrees to the long axis of the femur and the plate, the components parallel and perpendicular to the screw axis are $A_o = P \cos (158^\circ - \beta)$

and $B_o = P \sin (158^\circ - \beta)$ respectively. The axial load A to initiate sliding, was found to be governed by the perpendicular component of the applied load, B_o , the actual coefficient of friction (μ), and the length of the screw extending from the barrel (L_n). Maximizing the sliding capability of the sliding hip screw, therefore, required that the ratio of A_o/A be as large as possible.

It is then evident from the discussion that if the length of the screw extending from the barrel increased or the barrel length decreased, more resistance is required for sliding, and there is a substantial rise in the potential for jamming. The only way to reduce the risk of jamming is by engaging the screw deep into the barrel and thereby lengthening the lever arm (L_b).

2.3 Mathematical Analysis of Stress in the Human Femur

In order to calculate the stresses in the human femur, muscle forces acting at the femoral head have to be taken into account alongwith the body weight. By adding inertial forces to the body, there is an increase in the body weight by a multiplicative factor which also tends to increase the stresses acting on the femur by the same factor.

The muscles considered for the stress analysis in the femoral head region are the hip abductors and the tensor fasciae latae. These muscles are chosen because equilibrium requirements provide a range of values for their muscle forces. Other muscle groups such as ilio-psoas, the short hip rotators, the hip abductors and the gluteus maximus are active, but it is more difficult to evaluate values for

these muscle forces.

The major muscle groups of concern in the one-legged stance are the abductor group and the ilio-tibial tract. The latter is only in tension, above the greater trochanter, when the pelvis is in an extreme sagging position. The gluteus minimum and the gluteus medius muscles exert $3/4$ of the total abduction force M and are inserted into the greater trochanter. The gluteus maximus and the tensor fascia latae are inserted into the ilio-tibial tract below the greater trochanter. These two muscles supply $1/4$ th of the abduction force. Thereby the force T in the ilio-tibial tract is unlikely to be greater than $0.25M$.

The combined effect of force in the gluteus maximus, tensor fascia latae and ilio-tibial tract is an inward force on the lateral boundary of the greater trochanter, and is assumed to be distributed on the distal lateral trochanter surface. The head load was assumed to be distributed over a 60° arc on the femoral head.

The values for forces and the angles at which they act obtained by McLeish and Charnley for a body weight of 158 lbs. are

$$M=1061\text{N}, J=1620\text{N}, T=172\text{N}, \phi = 24.4^\circ, \theta = 29.5^\circ$$

Similarly Paul and Morrison have examined the mechanics of walking and estimated the muscle and joint forces acting on the femur. In the one-legged stance phase between the time interval from heel-strike through foot flat these results were evaluated. There are five stages in the walking cycle where the various muscle and joint forces peak almost simultaneously. These occur at 2%, 13%, 19%, 50% and

63%. The magnitude of forces as determined by Paul and Morrison for these five instances are listed in Table III.

The stress analysis on the femoral shaft in the past has been analyzed using the beam theory. An axial load of 165 lbs. was applied to the head of the femur, reacted by a force of equal magnitude and opposite direction at the distal end. For a man weighing 200 lbs., the axial load corresponds to the body weight less the weight of one leg. Results have shown that a maximum tensile stress in the shaft of the femur was 11.5MPa.

To maintain the one-legged stance the action of the hip abductor muscles have to be taken into consideration. The resultant force acting on the greater trochanter would create a moment to prevent rotation of the body about the hip joint. This force was estimated to be around 358 lbs. The addition of this force increases the axial compression in the femoral neck, giving a joint load of 525 lbs. at the head of the femur.

When the abductor muscle force was included by researchers the maximum tension in the femoral shaft was found to be 45.7MPa. This meant that the stress was increased four times the normal stress when the abductor muscle force was considered.

CHAPTER III

Biomechanics and Forces acting on the Hip-Joint

3.1 Biomechanics of the Hip:

Biomechanics is a basic science of orthopaedics utilizing the principles of Engineering Science in understanding mechanical dearrangements of the body. Biomechanics deals with motions and forces, and the interrelationships between them. Body movement is brought about by proper applications of these forces. These forces also have internal effects which produce a state of strain. The amount of strain and deformation the body will undergo depends upon its particular mechanical characteristics.

Biomechanics is sub-divided into four groups. The first group is involved with the mechanical properties of the tissue, concerned with basic tissues of cartilage, cancelous bone, cortical bone, etc. The study of substructure like the upper end of femur, hip joint and acetabulum forms the second domain. Kinematics the third sub-group deals with description of the motion of the whole joint, or of the motion on or about the joint surface. The fourth group deals with loading of the structure in use.

3.2 Forces acting on the Hip Joint

The hip joint is surrounded by large muscles and strong ligaments. The

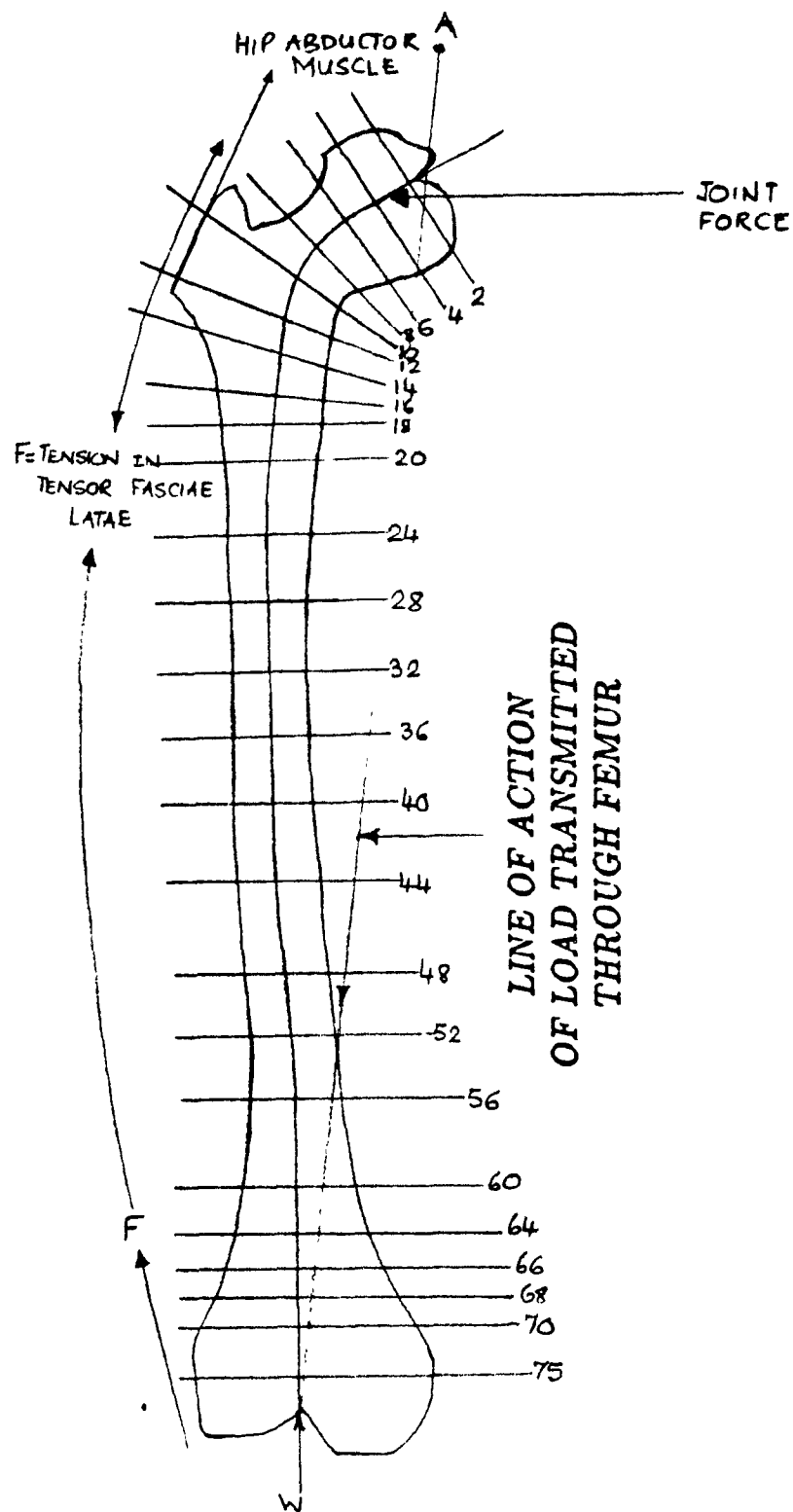


Fig. 9 Force Diagram of the Normal Femur

muscles, and to a certain extent, the ligaments affect and complicate the calculations of the forces which act on the head of the femur. Understanding the biomechanics of the hip joint has been rendered difficult because of lack of knowledge of the magnitude and direction of forces acting on the hip joint. Meyer suggested that the joint cartilage be subjected to a pressure which is determined by gravity and muscular force. Fick, Milch²⁸ and Debrunner pointed out the importance of muscular action on the hip-joint.

Many previous attempts have been made to calculate the resultant force acting on the head of the femur. Henke, Thomsen and Kuntscher suggested that both muscular and gravitational forces have to be considered, when calculating the forces acting on the hip-joint.

Pauwels felt that the center of gravity lies eccentrically in relation to the longitudinal axes of the bones and this may provoke heavy bending moments. Koch²⁶ calculated the dynamic load twice the value than that of the static load. In gait the static load on the head of the femur is about 80 percent of the body weight and the forces acting against the head of the femur will be 1.6 times the body weight. Koch pointed out, that the femur may act as a shock absorber due to flexion in the hip and the knee. Grunewald felt that due to muscle forces, the value of the force acting on the hip-joint may reach 900 lbs. Storck calculated the muscle force to be equal to twice the value of the body weight.

Pauwels on the basis of Fischer's works calculated the magnitude and

direction of the force acting on the head of the femur in a single-leg support, two-leg support and during the stance-phase in gait. The muscle forces in the horizontal plane were found to be negligible in both the single-leg stance and the two-leg support phase. While walking, a dynamic component is added in the horizontal plane. The dynamic component in the frontal plane is predominant. Pauwels believed that insignificant muscular forces act when standing on two legs, and the vertical force acting down is equal to one-third of the body weight.

In a single leg support, the muscular forces affect the magnitude and direction of the resultant force. The center of gravity for the superimposed body weight was assumed to be 109 mm. from the center of the head, and the lever of the abductor muscle was estimated to be at 40 mm. The force acting on the head of the femur will then be about three times the value of the total body weight. If consideration is given to the dynamic forces during the stance phase the forces will be about four and a half times the body weight. When using a walking stick, the vertical force can be reduced to approximately 1.7 times the body weight.

Other researchers Cabot and Peralba, Knese, Muller, Hackenbroch, Williams and Lisner, Hochman and Hauge found out that the force or load acting on a single-leg or in gait varied between four and six times the body weight.

The resultant forces will not be absolutely vertical because of the muscles. So far all the calculations have been made for the frontal plane. Storck felt that the force in the standing position on one leg forms an angle of 15° with the

vertical plane. Pauwels believed that standing on two legs results in a vertical force, because the muscular components are insignificant. The force in the frontal plane forms an angle of 16° with the vertical line. Pauwels also found that in the horizontal plane it forms a dorsally open angle with the frontal plane, of about 30° in the beginning of the stance-phase and at the end of the phase it reaches a minimum angle of 2° with the frontal plane.

Inman²⁴ thought that the direction of the force in one-leg support is constant, irrespective of the position of the pelvis. The force direction forms an angle of $10^\circ - 15^\circ$ with the vertical line in the frontal plane which corresponds to the direction of the medial trabecular system. The epiphyseal line runs perpendicular to the medial lamellae. As the resultant force seems to follow these trabeculae, no consequent shearing force will arise on the epiphyseal cartilage in the frontal plane.

The magnitude of the pressure arising on the head of the femur depends on the size of the contact surface. It is difficult to conclude exactly, since one cannot be certain that the center of the contact surface coincides with the point of force application. Fick thought that the medial upper portion of the head of the femur is subjected to the greatest pressure since its lateral position lies outside the acetabulum. Buchet and Castaing pointed out that the anterior part of the femoral head is of greater importance to the mechanics of the hip-joint. The resultant force runs along the longitudinal axis of the neck and forces the head of the femur upwards, inwards and forwards in the standing position.

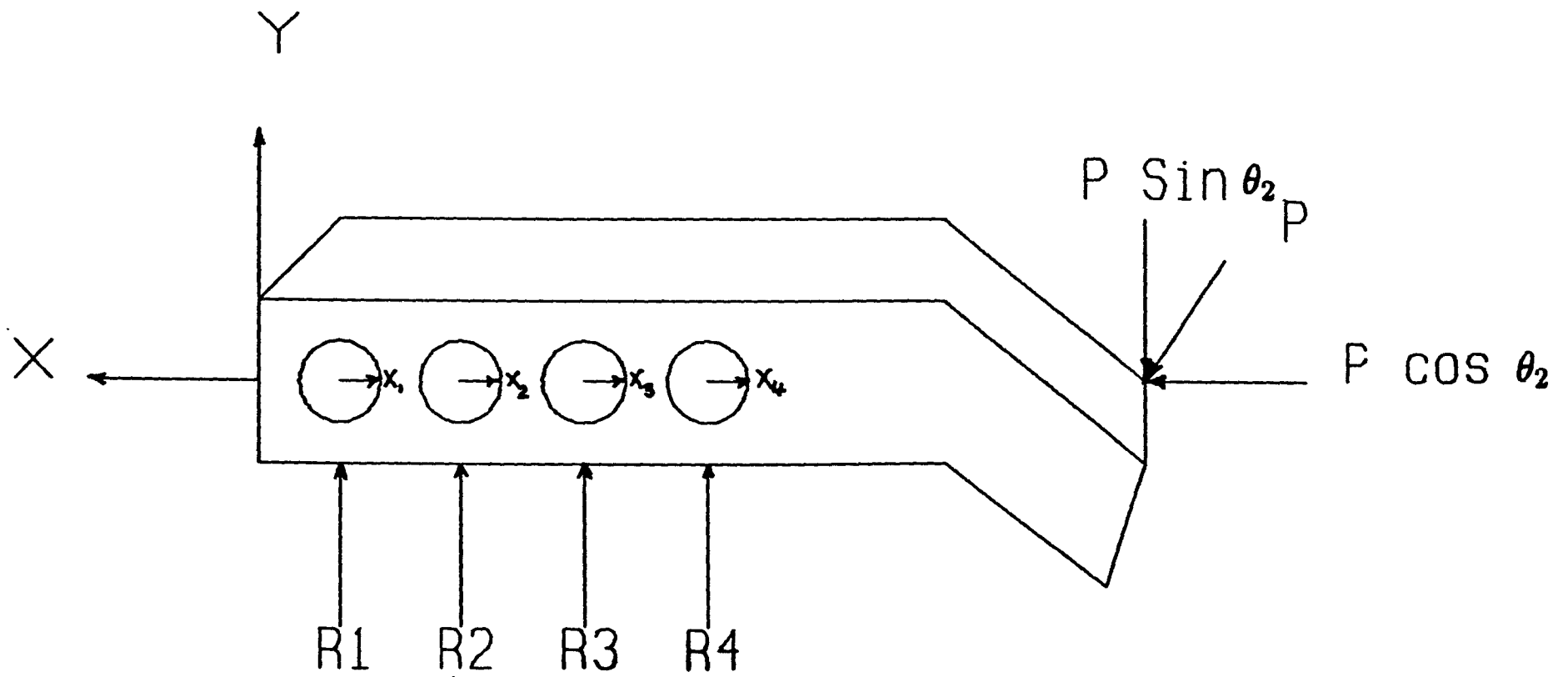


Fig:10 BEAM ANALYSIS OF PLATE ,

CHAPTER IV

SYSTEM MODEL

To calculate the stresses acting on the plate it is very essential to setup a Mathematical model based on the assumption that it is a solid beam having an uniform thickness. The plate can then be analysed by beam analysis method. The dimensions for the plate were obtained from the Manufacturers handbook. To compare the 135° and a 150° plate we first need to setup standard equations for the plate, such that it would give us approximate values of stresses, acting at different points along the entire length of the plate.

Nomenclature

θ_1 = Angle of plate (135° or 150°)

θ_2 = Angle at which force P acts = 24.4°

l_1 = length of the plate

l_b = length of the barrel

P = Load or force transmitted by bone

E = Modulus of Elasticity

= 200×10^3 MPa for 316L S. S.

= 240×10^3 MPa for Co Cr Mo S

= 100×10^3 MPa for Ti (ASTM-F67)

M = Bending Moment

y = deflection

I = moment of inertia

Z = section modulus

$$\sigma = \frac{M}{Z}$$

Assumptions:

- [1] The plate is assumed to have an uniform cross-section.
- [2] Previous results have proved that the plate bends at the first hole hence all forces are assumed to be concentrated at the first hole and none are transmitted beyond the first hole.
- [3] No moments are assumed at the four holes.
- [4] The holes for the bolts are assumed to be equidistant.

$$\sum X = X_1 + X_2 + X_3 + X_4 - P \cos \theta_2 = 0 \quad (4.1)$$

$$\sum Y = R_1 + R_2 + R_3 + R_4 - P \sin \theta_2 = 0 \quad (4.2)$$

$$\sum M = R_2 l + R_3 2l + R_4 3l - P \sin \theta_2 (l_1 + l_b \cos \theta_1) - P \cos \theta_2 (l_1 + l_b \cos \theta_1) = 0 \quad (4.3)$$

$$\begin{aligned} \sum M_z(x) &= EI \frac{d^2 y}{dx^2} \\ &= R_1 x + R_2(x - l) + R_3(x - 2l) + R_4(x - 3l) + (X_1 + X_2 + X_3 + X_4)(x - l_1) \tan \theta_1 \end{aligned}$$

Integrating once we get,

$$EI \frac{dy}{dx} = R_1 \frac{x^2}{2} + C_1 + R_2 \frac{(x - l)^2}{2} + R_3 \frac{(x - 2l)^2}{2} + R_4 \frac{(x - 3l)^2}{2}$$

$$+(X_1 + X_2 + X_3 + X_4) \frac{(x - l_1)^2}{2} \tan \theta_1$$

Integrating further

$$EIy = R_1 \frac{x^3}{6} + C_1 x + C_2 + R_2 \frac{(x - l)^3}{6} + R_3 \frac{(x - 2l)^3}{6} + R_4 \frac{(x - 3l)^3}{6}$$

$$+(X_1 + X_2 + X_3 + X_4) \frac{(x - l_1)^3}{6} \tan \theta_1$$

We have the following unknown variables

$$R_1, R_2, R_3, R_4, X_1, X_2, X_3, X_4, C_1, C_2$$

$X_1 < X_2 < X_3 < X_4$. The shearing force applied to the plate at each hole can be calculated since each is a function of X_4 in terms of a constant k . k is calculated by the formula

$$k = \frac{n - n'}{n}$$

where n = Total no. of screws

n' = Total no. of screws in the rows between the row being checked in tension and external load.

To find displacement at $x=0$, $x=l$, $x=2l$ and $x=3l$

$$\delta_{x=0} = 0$$

$$\delta_{x=l} = 0$$

$$\delta_{x=2l} = 0$$

$$\delta_{x=3l} = 0$$

Substituting $X_1 = k_1.X_4$, $X_2 = k_2.X_4$, $X_3 = k_3.X_4$ where ($k_1 = \frac{1}{4}$, $k_2 = \frac{1}{2}$, $k_3 = \frac{3}{4}$) and the conditions for displacement in equation for Ely we get,

$$\delta_{x=0} = 0 = C_2 \quad (4.4)$$

$$\delta_{x=l} = 0 = R_1 \frac{l^3}{6} + C_1 l \quad (4.5)$$

$$\delta_{x=2l} = 0 = R_1 \frac{(2l)^3}{6} + C_1 2l + R_2 \frac{l^3}{6} \quad (4.6)$$

$$\delta_{x=3l} = 0 = R_1 \frac{(3l)^3}{6} + C_1 3l + R_2 \frac{(2l)^3}{6} + R_3 \frac{l^3}{6} \quad (4.7)$$

We have 7 unknowns and 7 equations, solving them we can get values for all unknown parameters.

For bending stresses we know that

$$\frac{M}{I} = \frac{\sigma}{y} = \frac{E}{R}$$

but

$$\frac{I}{y} = Z = \text{section modulus}$$

Therefore,

$$\sigma = \frac{M}{Z}$$

For a beam with uniform cross-section

$$I = \frac{bh^3}{12}$$

and

$$Z = \frac{bh^2}{6}$$

Therefore,

$$\sigma_{x=l_1} = f(P, \theta_1, \theta_2, \dots)$$

We also know that $\sigma_{real} = \sigma_{calc.} \times k$

where k=stress concentration factor found from tables.

Solving the equations simultaneously we have the following values:

$$X_1 = 0.25X_4, \quad X_2 = 0.50X_4, \quad X_3 = 0.75X_4$$

$$\sin \theta_2 = 0.413, \quad \cos \theta_2 = 0.9106 \quad \& \quad l_b = 38mm$$

For a 135° plate

$$\cos \theta_1 = 0.707$$

$$X_4 = 0.364P$$

$$C_1 = -R_1 \times \frac{l^2}{6}$$

$$R_1 = \frac{P}{5.l_1 + 134.35} \times 0.084l_1 - 68.88$$

$$R_2 = -6.R_1$$

$$R_3 = 4.R_1$$

$$R_4 = R_1 + 0.413P$$

$$l = l_1 + 26.87$$

Similarly using the same values for X_1, X_2, X_3, θ_2 and l_b for a 150° plate we get the value of R_1

$$R_1 = \frac{P}{5.l_1 + 134.35} \times [0.094l_1 + 10.575]$$

Knowing the values of the variables like P and l_1 we can find the value of the unknowns like $R_1, R_2, R_3, R_4, X_4, C_1$. Substituting these unknown values in the formula for moments at different lengths we get

$$M_x = 0 \text{ for } 0 < x < l$$

$$M_x = R_1.x + R_2(x - l) \text{ for } l < x < 2l$$

$$M_x = R_1.x + R_2(x - l) + R_3(x - 2l) \text{ for } 2l < x < 3l$$

$$M_x = R_1.x + R_2(x - l) + R_3(x - 2l) + R_4(x - 3l) \text{ for } 3l < x < l_1 - 3l$$

Using the moment equations listed above for various values of x we get values of moment for $P = 250$ N and plate angle $= 135^\circ$ at $x = 15$ mm, 30 mm, 50 mm the values of M_x are -13,274 N-mm, 4852.63 N-mm and -75,243.66 N-mm.

To calculate stress we use the formula

$$\sigma_x = \frac{M_x}{Z}$$

The corresponding values of stress for $b = 18$ mm, $h = 10$ mm are -44.24 N/mm^2 , 16.175 N/mm^2 and -250.81 N/mm^2 .

Similarly for a 150° plate the stresses for similar values of x are found to be 29.103 N/mm², -10.88 N/mm² and -255.05 N/mm².

Summary:

From the above discussion it can be concluded that a mathematical model (from the given set of equations) is developed for the plate. Stresses at various cross-sections can be found using the mathematical model. Using stress charts we are able to calculate real value of stress. These values when plotted on a graph helps us to compare the behavior of the two plates.

CHAPTER V

Computer Aided Design and Finite Element Modeling

Introduction:

Computer Aided Design (CAD) is used to graphically simulate a design problem. There are various software packages available like Autocad, Versacad, etc. Software packages like I-DEAS (Geomod) is used to create an object model before an analysis is done on the two- dimensional or three-dimensional model to calculate stresses, displacement, etc.

5.1 Basic Classification of CAD System

Generally, any CAD system can be reviewed as a combination of two major functional components, mainly Design/Modeling and analysis.

In the Design/Modeling components, the system can be designed and modeled with basic data available to the designer. Here, with help of extensive menus the designer can develop the required system on the screen. Depending on the application, the user can also use the optimization software and 2-D or 3-D modeling system to develop it.

The second component of any CAD system is the analysis module. Depending on the CAD software used, and the area of application, the user can have different analysis modules such as a dynamic analysis module, finite element analysis module, etc. Here, the system which is designed and modeled by designer

is put under various tests through analysis to check the design behavior. In some of the software, this component is optional and the users have an option to choose from various analysis software packages available on the market. In such cases the user should be cautious in checking the compatibility of the analysis module with modeling module.

5.2 Classification of CAD based on Dimension

All CAD software can be broadly classified into the three categories, based upon the dimension it handles, viz.

- [i] 2-D, Two dimensional: CAD software treats the flat object. These are generally called drafting software.
- [ii] 2 1/2-D, Two and one-half dimensional: This type of software is just an extension of 2-D software, i.e. it can handle three dimensional objects without side details.
- [iii] 3-D, Three dimensional: Treats 3-D objects with more complex geometries. Most of these software packages are capable of computing physical properties like mass, volume, inertia etc.

5.3 Classification based on Computer Hardware System:

CAD software can also be classified based on the computer system on which it runs. The classification of computer systems is based on data processing approach, speed, accessible memory and cost. Both speed and memory depend mostly on word length, the number of bits a computer can handle at a time, that is 16 bit, 32 bit, etc. The main factors which dominate the processing speed and

amount of main memory that can be accessed are internal word length and external word length.

All CAD systems can be classified into three categories.

- [a] PC based CAD system: Most of the 2-D modelers can easily be run today on PC's without any extra hardware. Although many 3-D modelers running on PCs are as sophisticated as those available for large computers, wireframe/ surface modelers are a good fit for the PCs. This is true because they do not require as extensive computing-power of a computer, as is required by a solid modeler. Indeed, with a 30386 microprocessor based PC, wireframe/surface modeling can be almost as interactive as 2-D drafting. Most of the 3-D solid modeler perform functions such as shading to make a model appear realistic, section analysis for mass and inertia properties. These require intensive computation and time consuming operations, hence require increased power of PCs.
- [b] Workstation based CAD System: The popularity of Workstation based CAD systems is increasing day by day due to their powerful graphic capability and large memory storage. Workstations consist of three basic components, a primary processor and associated memory, a graphics display system and software. Networking ability is another element which is often found in Workstations.

Workstations typically place an emphasis on graphics display and manipulation, since this is an effective method of off-loading the host. The features of a display system are directly related to the power of a display driver and not to

the characteristics of the terminal screen itself. Functions such as colorfill, line, arc generation and rotation are controlled by this display processor and associated with hardware.

- [c] Mainframe based CAD System: The word mainframe is used to denote a large central processing unit or centralized computer system that can support more than one workstation and peripheral devices and can drive printers, tape drives, etc. Memory is important since mainframes are used in data-intensive tasks.

5.4 Classification of CAD System based on Application:

Major applications include CAD for Mechanical Engineering (MCAE), CAD for Electronics Engineering (ECAD), Petroleum exploration and mapping, Computer Aided Software Engineering (CASE), Bio-Medical Engineering Systems and Architecture, Engineering and Construction (AEC).

5.5 Classification of CAD System based on Operating Systems:

A CAD system uses different levels of software, these are an operating system, an application package and command language. An operating system is a computer program or collection of programs. The main function of an operating system is to access information and programs on auxiliary storage and other types of input or output devices. An operating system contains a file manager which keeps track of and handles information of files. The operating system takes the steps necessary to acquire the information and complete the task. It will do what is requested and places the result where instructed. In general, to control the

execution of other programs and to control the flow of data are the two basic functions of any operating system.

The two main operating systems in use today, are Disk Operating System (DOS), and UNIX. The recent trend is more towards UNIX, hence more and more CAD systems are offering both UNIX as well as DOS option. More and more workstations and PCs now adopt architectures, which allow them to run on almost all CAD systems.

5.6 I-DEAS (Integrated Design Engineering Analysis System):

I-DEAS is an integrated package of Mechanical Engineering software tools to help facilitate a concurrent engineering approach to Mechanical Engineering Product Design. I-DEAS allows the different groups in a Company to access the same data and exchange information freely.

I-DEAS is made up of a number of “families” of products, each subdivided further into “modules” all executed from a common menu, and sharing a common database. (A module equals one computer executable program). The main families are Solid Modeling, Engineering Analysis, System Dynamics, Test Data Analysis, Drafting and Manufacturing.

5.7 Solid Modeling:

Solid Modeling contains the modules of Object Modeling and System Assembly. Together they are referred to as “Geomod”. Object Modeling is the place where the geometry is actually defined. Geometry is represented as a solid, as

contrasted with surface or wire frame model programs. The created geometry can be used for mass and inertia property calculation, interference studies, Finite Element Modeling, Manufacturing.

To create a geometry the simplest method is to use primitive shapes such as blocks, cylinders, cones and spheres. More complex shapes can be made by extruding and revolving profiles. Use of skinning operation is done for complex structures which forms surfaces between different profiles. Joining or cutting objects is done using an object boolean operation.

System Assembly module allows building complex systems out of objects defined in Object Modeling. These systems can be used for visualization, mass properties calculation, interference studies.

5.8 Engineering Analysis:

Engineering Analysis family is used to convert geometry into a Finite Element Model which in turn is used to analyze the effects of structural and thermal loads. The Pre/Post module is used to create the model and define the loads. The Model solution is then used to calculate the results from static, thermal or normal nodes analysis, which are redisplayed in the Pre/Post module.

Geometry created in Object Modeling can be used directly in Engineering Analysis or geometry can be created directly in Engineering Analysis. For sculptured surfaces or complex intersection of surfaces it is preferable to generate the geometry in Object Modeling.

Optimization module can be used to run several iterations to optimize a design to find optimum thickness parameters to minimize the weight, given various load cases.

5.9 System Dynamics:

For those problems that require vibration analysis, I-DEAS system dynamics can be used to perform linear vibration analysis on dynamic system module. Vibration can be studied in the time domain (transition analysis) or in frequency domain.

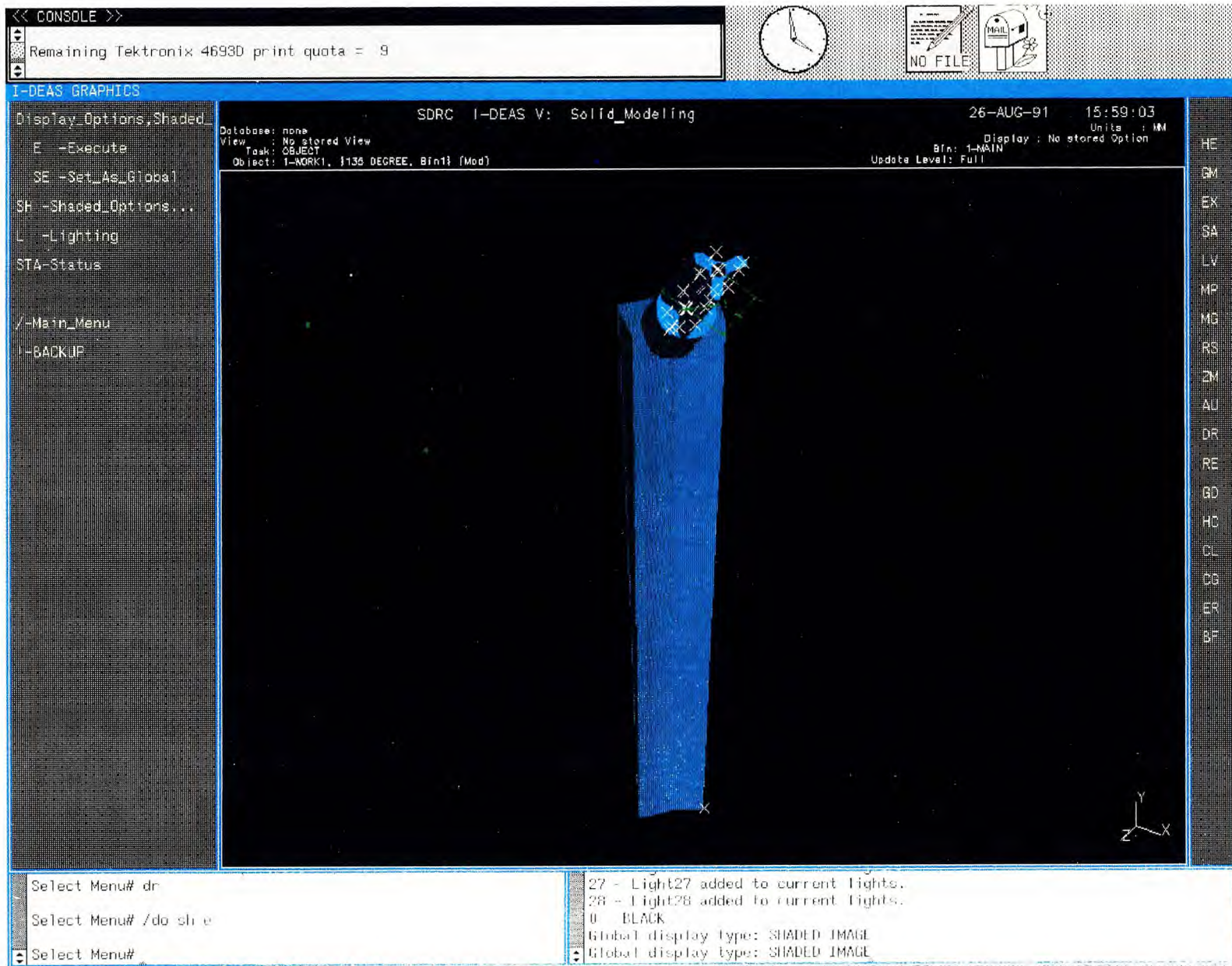
5.10 Test Data Analysis:

The goal in the Mechanical Computer Aided Engineering (MCAE) design process is to use testing through developmental cycle, and to make better use of the test data through more advanced analyses techniques and better integration with other disciplines. Initial test might be done on a prototype or previous design to understand the load environment and to develop loads for a finite element model.

Emphasis in I-DEAS test data analysis is to make graphic representations of the numeric results in the form of 2D or 3D plots in various wire, bar or surface displays, or to display information directly on the geometry of the structure being tested.

5.11 Methodology:

In order to analyze the two plates, the I-DEAS software package is used. First we have to make a solid model in the Solid Modeling Task. The shape of the



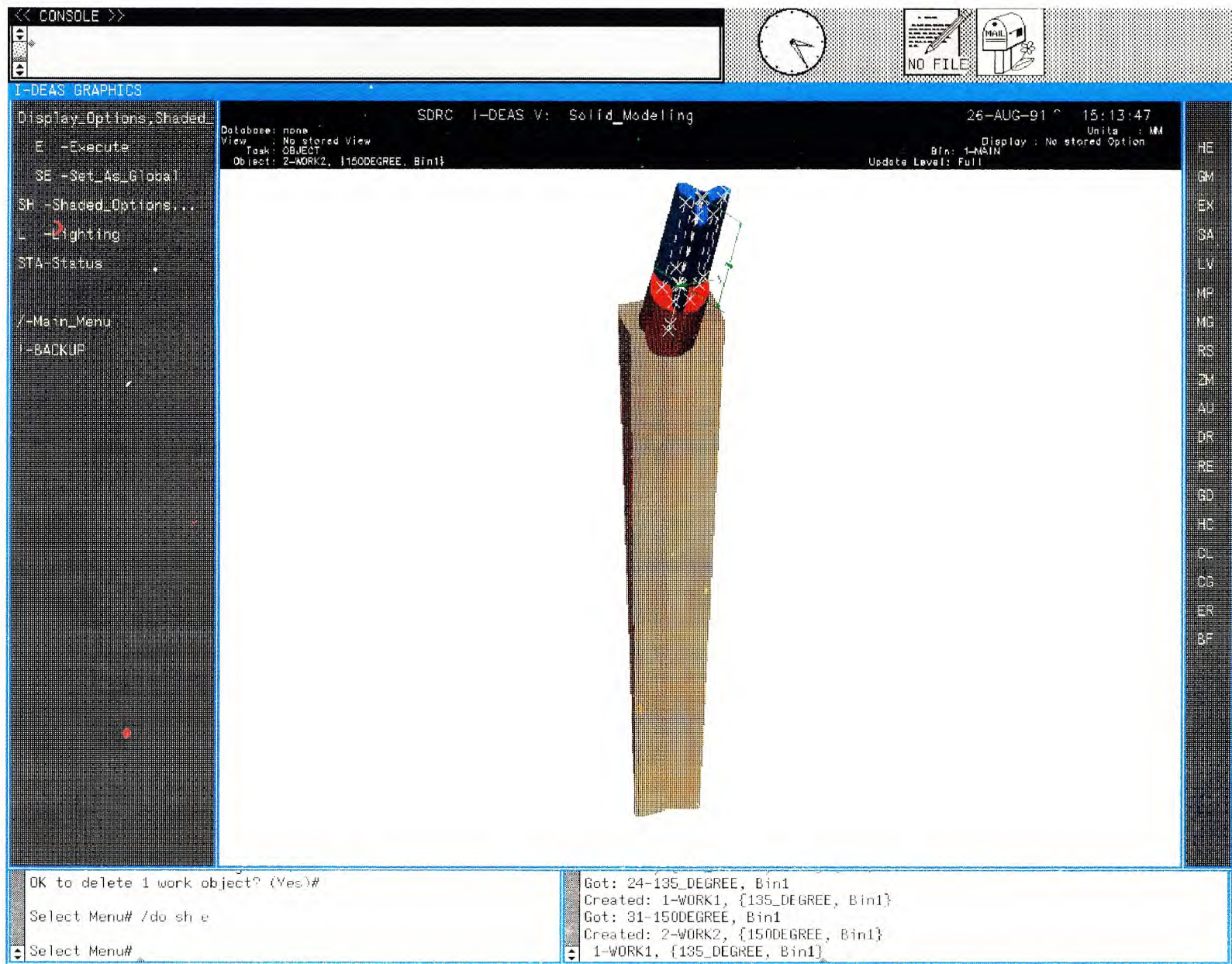


plate makes it difficult for us to make one complete solid model. Hence, we have to determine a way to divide the model into different parts. Because of the complex shape of the plate we divide the plate into three different parts. We store each part separately, and later use the *JOIN* task to construct a solid model of the 135 and 150 degree plate.

The stem which is the first part is made by the “skinning” operation of two profiles. The end or the third part of the plate is created by extruding the profile in the Z-direction. The second or the middle portion of the plate is cylindrical and is joined with the end part by the “Boolean Join” operation. Finally the complete solid model is constructed by joining the two sub-parts. The joined second and third part is then bent at the desired angle. Holes are created in the stem using the Boolean cut operation.

We have to check for various errors like interference, overlapping geometry, etc. As soon as the solid model is created, it is ready for finite element analysis.

We go to the Finite Element Analysis Task and get the object from the stored object menu. Having recalled the object from the stored Solid Modeling Menu, we first create the Mesh areas for the plate. If there are any errors like incomplete loop, etc. we correct the errors. If we are able to create a complete mesh area for the various curves, our model is then ready to undergo transformation to one solid volume or various volumes. This is done to enable the software to generate nodes and elements in the Mesh Generation Task of the Finite Element

Analysis Menu.

Once the mesh volume/volumes are created either manually or automatically, we go to Mesh Generation Menu and pick the Solids Menu from it to generate nodes and elements for the Mesh volume. Having generated the nodes and elements, we store the nodes and elements. The list shows us exactly how many nodes and elements are generated and stored.

Having created the nodes and elements we write the workset to the ANSYS universal file. Using the ANSYS package we define the constraints, the nodes at which the forces will act. Once loading is done we check for any errors that might occur because of overlapping nodes and elements. We then generate the output file where we determine the values for nodal forces, displacements, shear stresses at the constraints and various nodes and elements.

CAD SOFTWARE FEATURES AND ANALYSIS

5.12 2-D CAD Software:

Such software, is generally called drafting software, is most popular in industry due to the drafting capability, low cost and less demanding hardware requirements. It accounts for a major portion of the total CAD market.

There are four essential functions required by any drafting software. These are geometry creation, geometry editing, dimensioning and labeling, and input as well as output on peripherals. Geometry creation is the construction of a shape on the screen, using a set of standard elements which generally include points, lines,

arcs, circles, polygons etc. Generally, under “Draw” option, users are provided different options. Users are also able to insert the text in the design. For editing the geometry, the software provides basic options like “Erase” or “Remove” alongwith various options for visualization of the geometry like scaling to smaller image or bigger image, rotation in the 2-D plane, copying option, option for translation of geometry, etc.

While editing the geometry the software should allow the user to edit part of the object by providing options like “Explode” or “Divide”, which divides the geometry into a number of parts and then the user can edit the part required by the design. Also the software should provide the option for enclosing the required area of a drawing for translation or rotation of a group of lines, points or polygons. Also, options for filleting, chamfering, trimming should be provided to generate the design more precisely. For ease of creation of geometry, the software should have such options as “Orthogonal lines”, “Reference Axis”, “Grid layout”, etc.

Dimensioning and labeling are also very important features. Dimensioning should include the use of super and subscripted text along with inside and outside dimensioning techniques, depending upon the space availability. Also, software should have “ auto-dimensioning” option for ease of dimensioning and precision of drawing. The software should provide all these facilities associated with dimensioning.

For input/output of generated drawings the software should support dif-

ferent digitizers, mouse, keyboard, printers, plotters, etc. which are commonly available in the market.

5.13 **3-D CAD Software:**

Such software deals with three dimensional objects with side-view details of it. To deal with complex geometry and the inertial and sectional properties, such software uses various modeling methods.

A. 3-D Modeling Methods:

There are various methods for 3D modeling of an object. All 3D softwares use some of these methods to arrive at 3D modeling of any design. Following is a list of the modeling methods.

(i) Wireframe Modeling

(ii) Surface Modeling

(iii) Solid Modeling

[a] Instancing scheme

[b] Spatial Occupancy Enumeration Scheme

[c] Cell decomposition scheme

[d] Sweep method

[e] Constructive Solid Geometry

[f] Boundary representation scheme

[g] Hybrid scheme

B. Essential requirements of a 3-D Software:

The basic capabilities of a 3-D software includes:

- (i) An option to create a 3-D geometry with various techniques
- (ii) An option to edit the created geometry and check the physical properties
- (iii) An option for file utilities.

5.14 Hardware Support for 2-D and 3-D CAD Software:

a. Memory Devices:

Memory devices are needed for the software to reside and to store the work done on the system. There are two type of memory devices. Primary storage devices are used for two type of memory, Random Access Memory (RAM) and Read Only Memory (ROM). ROM is used for storage of an Operating System. The part of RAM is used for storage of an application program, and the remaining portion of RAM is available for the user to store his work on the system. The size of memory referred in the commercial market is RAM.

The secondary storage can be thought in terms of disk drives. With the help of these drives, user can increase the memory storage capacity, in the range of 16K bytes to 1M bytes. With the help of a secondary storage, user can work with the complex CAD software package. The access time will be high and so the speed at which different operations are performed will be low.

Hardware used in SUN Micro Lab:

VENDOR	SUN MICROSYS. INC. Sun 3/60
Operating System	Sun OS
Memory (RAM)	8-32 MB
Resolution	1150×900
Disk Less Remote Boot	Yes
CRT Size	19 Inches
Colors	256
Input Device	Mouse & Digitizer
CPU	Motorolla-68020
Processing Speed	25 MHz

Some of the available tools of Sunview include:

Command Tool

Shell Tool

Text Editor - Font Editor

Icon Editor

Mail Tool

Debug Editor

Clock

Lockscreen

b. Input Devices:

[i] Digitizer

[ii] Mice

5.15 ANALYSIS SOFTWARE:

The analysis software is used to test various stresses, strains, loads, etc. before it is put into operation. The conventional method of analysis is restricted to mathematical formula and the data available from that. With the development of CAD techniques, conventional analysis is replaced by an on screen analysis of component through various stress-strain criterion, and the sophisticated output results in terms of the different levels of loads, stress, strain, etc.

There are many analysis software available in the market. These are Finite element analysis (FEA), Dynamic analysis, Mechanism analysis, etc. The most popular analysis software is finite element analysis software. Since the work done in the thesis is related to FEA, we shall restrict the discussion in this section to finite element analysis software.

5.15.1 Capabilities of an FEA Software:

The finite element analysis is based on arrays of large matrix equations that can only be realistically solved by a computer. Most often FEA is performed with commercial programs.

The finite element method is applicable in several types of analysis. The most common is static analysis, which solves for deflections, strain and stresses in

structure under a constant set of applied loads. In most of the cases the material of a designed part is assumed to be linear elastic, but nonlinear behavior such as plastic deformation, creep and large deflections can also be analyzed.

Heat-transfer analysis can solve steady state and transient heat transfer problems. In most cases, the thermal output data are applied as an input to the structural analysis problem to determine thermal deflections and stresses.

The natural frequency analysis calculates the free vibration natural frequencies and associated mode shapes of a structure. This analysis used to predict the critical operating conditions for the machines.

The transient-dynamic analysis determines the time response history of a structure, subjected to a forced displacement function. Here the structure may behave linearly or in some cases friction, plasticity, large deflection or gaps may produce nonlinear behavior.

5.15.2 General Structure of an FEA Software:

All most all FEA Software are made up of three modules. These modules are Preprocessor, Model Solution and Postprocessor.

In preprocessor module, user can define the geometry and construct the mesh by defining the nodes, elements and surfaces. Most of the preprocessors ostensibly free the user of many routines, or otherwise time consuming tasks in constructing the mesh by offering the options such as automatic mesh generation, mesh copying, element reflection, etc. Accuracy of the mesh generation depends

on the type of geometry used for the basic construction. The time required in mesh generation depends on the type of geometry, number of elements and the processing speed of a computer. Generally, finer the mesh, more accurate the result of the analysis. After mesh generation, the model is defined with the actual load conditions.

Once the geometry is defined with the mesh and load conditions, the model is submitted to the model solution module. Depending on the software used, this module will solve the model with different techniques. Modern FEA software provides an option for the user to choose third party's solution module for the fast and accurate results.

The postprocessor module simplifies the interpretation of results by displaying the output data graphically. In case of conventional method, the results of analysis appears in the tabular form without any graphics. The output display may be in the form of contour stress plots, deformed geometry with undeformed geometry on it.

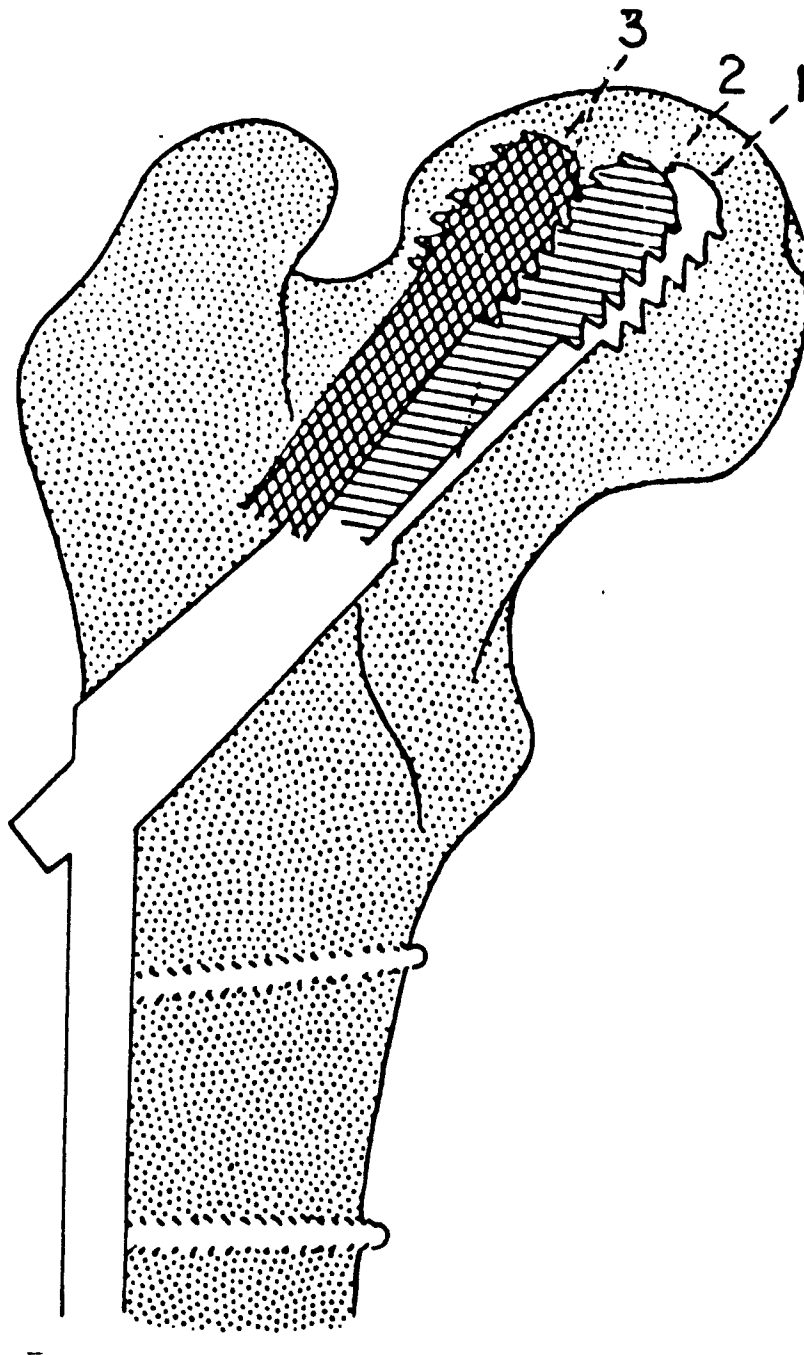


Fig. 13 Classification of screw position in femoral head

CHAPTER VI

CONCLUSIONS

The placement of the fixation device in the subarticular region of the femoral head provides the most satisfactory hold. It has been proved that a nail parallel to the main weight-bearing seams in the femoral neck, provides the best protection against movement of the screw within the neck. The stability of the comminuted fracture is dependent on its ability to impact, without causing the screw to break or cut out. There are three positions (Fig. 11) which are very important for the right placement of the screw.

1. The center of the screw tip lying on the center line of the femoral head or within half the diameter of the screw from it.
2. The center of the screw tip lying between half a screw diameter and one screw diameter from the center of the head.
3. The center of the screw tip lying more than one screw diameter from the centerline of the femoral head.

The depth of penetration is evaluated by the distance of the end of the screw from the articular surface of the femoral head, as measured by the number of screw turns necessary before penetration of the joint would have occurred. The

screw normally advances by $1/8$ th of an inch on every turn. The third position is invariably associated with subsequent movement of the screw within the head. In positions 1 and 2 the screws with a penetration of $1/2$ an inch never moved. In the anteroposterior plane(position 3), alongwith position 2 in the lateral plane possibly allowed movement but no screw cut out. This clearly indicates how critical it is for the proper placement of the fixation device. If the screw is incorrectly placed, suitable precautions against undue stress should be taken after placement. Weight bearing on the fracture should be discouraged until union has occurred. Repeated attempts at achieving perfect screw placement can lead to serious medical complications.

Placement of the 150° plate is difficult to achieve than the 135° plate because of its high angle. The 150° plate occupies a rather high position in the head, and since it enters the shaft below the fracture site in rather thick cortical bone, the angle of entry has to be exact. The bone in the cortical region is too thick to permit any crushing, to correct minor errors of the angle of insertion, hence for routine purposes a 135° plate is recommended. The 150° plate should be used in those fractures, in which the lesser trochanter calcar fragment is so large, that considerable medial displacement and shortening are necessary to achieve stability. The 150° plate in this position allows the fracture to be placed in valgus, the screw entering the proximal fragments, through the open medulary cavity, and being

correctly placed centrally within the head. This valgus position compensates for the inevitable shortening. Despite the theoretical mechanical advantages associated with a 150° plate, the 135° proves easier to use and allows impaction well.

Solving the simultaneous equations by using the *Mathematica* software package the values of the unknown variables like the reaction forces $R_1, R_2, R_3, R_4, X_4, \sigma_{calc.}$, etc. can be found. Varying the values of these different variables alters the value of stress. The results from the Mathematical Model indicate that the 150° plate is superior from the mechanical point of view because of the high angle and strength.

Using the FEM Model we are able to conclude that the assumptions made in the mathematical model hold true. Using the ANSYS software package we are able to calculate the value of stresses and displacements at various nodes and elements in the two plates. The values calculated for the first hole for the 135 degree plate are as follows:

$$\sigma_x = 2.473N/mm^2, \sigma_y = 0.78433N/mm^2 \text{ and } \sigma_z = 0.20139N/mm^2.$$

The displacement at the first hole U_x, U_y and U_z are equal to zero, since the constraints are applied at the holes.

Similarly the values calculated for the 150 degree plate are:

$$\sigma_x = 0.172595N/mm^2, \sigma_y = -0.412328E - 01N/mm^2 \text{ and } \sigma_z = -0.306374N/mm^2,$$

displacements U_x , U_y and $U_z=0$. From the results we can conclude that from the engineering point of view the 150 degree plate has lower stress values at the constraints, and is superior to the 135 degree plate. It is then recommended to use a compromise angle between 135° and 150° plate to have lower stresses and to ease the method of plate insertion.

σ_z v/s X
For 135° plate

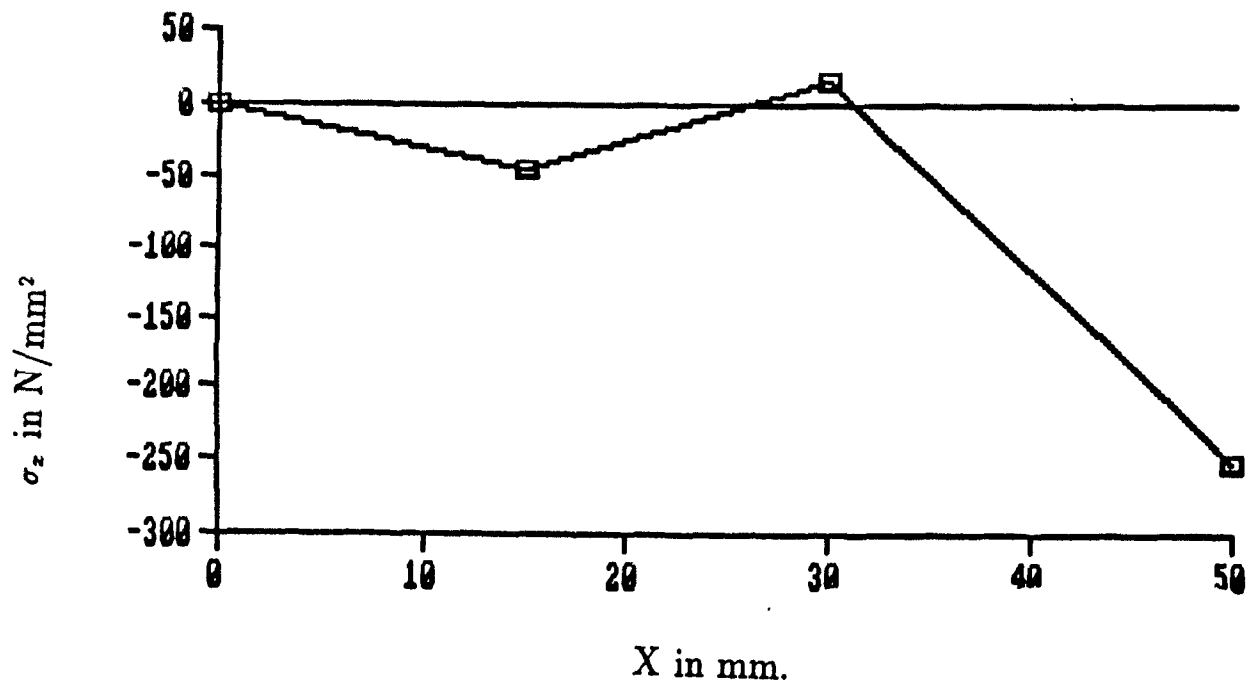


Fig. 14. Plot of σ_z v/s ' X ' for 135° plate

σ_x v/s X
For 150° plate

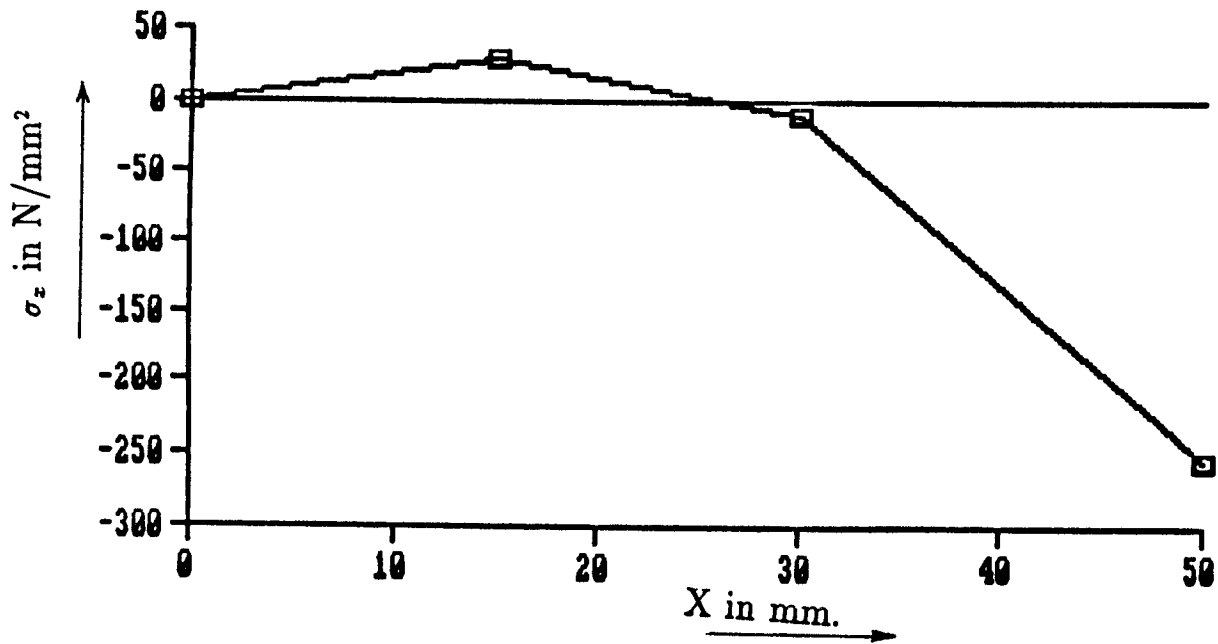


Fig. 15. Plot of σ_x v/s ' X ' for 150° plate

CHAPTER VII

BIBLIOGRAPHY

- [1] Boyd, H.B. and Anderson, L.D., "Management of Unstable Trochanteric Fractures," *Surgery, Gynecology and Obstetrics*, **112**:633-638, 1961.
- [2] Brekelmans, W.A.M., Poort, H.W. and Sloof, T.J.J.H., "A new method to analyse the mechanical behavior of skeletal parts," *Acta Orthop. Scand.*, **43**: 301-317, 1972.
- [3] Brown, T.D. and Ferguson, A.B., "The development of a computational stress analysis of the femoral head", *J. Bone Jt. Surg.*, **60-A**:619-629, 1978.
- [4] Brown, T.D., Way, M.E. and Ferguson, A.B., "Stress transmission anomalies in femoral heads altered by aseptic necrosis," *J. Biomechanics*, **13**:687-699, 1980.
- [5] Brown, T.D., Mutscher, T.A. and Ferguson, A.B., "A non-linear Finite Element analysis of some early collapse processes in femoral head osteonecrosis," *J. Biomechanics*, **15**:705-715, 1982.
- [6] Carter, D.R., Vasu, R., Spengler, D.M. and Dueland, R.T., "Stress fields in the unplated and plated canine femur calculated from in vivo strain measurements," *J. Biomechanics*, **14**:63-70, 1981.

- [7] Chand, R., Haug, E. and Rim, K., "Stresses in the human knee joint," *J. Biomechanics*, **13**:185-190, 1976.
- [8] Chao, E.Y. and An, K.N., "Perspectives in measurements and modeling of musceloskeletal dynamics," *Biomechanics-Principles and applications 1-18*, *Martinus Nijhoff, The Hague*, 1982.
- [9] DePalma, "The management of fractures and dislocations," 1250-1258.
- [10] Dimon, J.H. and Hughston, J.C., "Unstable Intertrochanteric Fractures of the hip," *J. Bone and Jt. Surgery*, **49-A**:, 440-450, April 1967.
- [11] Evans, E.M., "Treatment of trochanteric fractures of the femur," *J. Bone Jt. Surg.*, **31-B**:, 190-203, 1949.
- [12] Frankel, V.H., "Bio-mechanics of the Hip," **5**:, 105-125, 1972.
- [13] Frankel, V.H., "The femoral neck: function, fracture mechanism and internal fixation-an experimental study," *Springfield, Ill.*, 1960.
- [14] Garden, R.S., "The structure and function of the proximal end of the femur," *J. Bone Jt. Surg.*, **43-B**:, 576-589, 1961.
- [15] Garden, R.S., "Low-angle fixation in fractures of the femoral neck," *J. Bone Jt. Surg.*, **43-B**, 647-663, 1961.
- [16] Ghassemi, F., Tabie, S., Tarr, R., Harris, L. and Clarke, I.C.,
 "Intertrochanteric fracture fixation model using three-dimensional non-linear Finite Element Analysis," *Proceedings 27th Annual Meeting Orthopaedics*

- Res. Soc., 104, ORS, Chicago, 1981.
- [17] Gluckmann, A., "The role of mechanical stresses in bone formation in vitro," *J. Anat.*, 231-239, 1941-1942.
 - [18] Hassler, C.R., Rybicki, E.F., Cummings, K.D. and Clark, L.C., "Quantification of bone stresses during remodeling," *J. Biomechanics*, **13**:, 185-190.
 - [19] Haughton, S., "Notes on animal mechanics, on the muscular mechanism of the hip-joint in man," *Med. Times Gaz.*, 638-641, 1864.
 - [20] Hayes, W.C., Snyder, B., Levine, B.M. and Ramaswamy, S., "Stress morphology relationships in trabecular bone of the patella," *Finite Element in Biomechanics* (edited by Gallagher, R.H., Simon, B.R., Johnson, P.C. and Gross, J.F.), 223-268, J.Wiley, New York, 1982.
 - [21] Holt, E.P., "Hip Fractures in the trochanteric region," *J. Bone Jt. Surg.*, **45-A**, 687-705, June 1963.
 - [22] Huiskes, R., Janssen, J.D. and Sloof, T.J., "A detailed comparison of experimental and theoretical stress analysis of a human femur," *Mechanical properties of Bone AMD*, **45**:, 211-234, ASME, NY, 1981.
 - [23] Huiskes, R. and Chao, E.Y.S., "A survey of Finite Element Analysis in Orthopaedic Bio-mechanics, The first decade," *J. Biomechanics*, **Vol. 16 No. 6**:, 385-409, 1983.
 - [24] Inman, V.T., "Functional aspects of the Abductor Muscles of the Hip," *J.*

- Bone Jt. Surg.*, **29**:607-619, July 1947.
- [25] Jewett, E.L., "One-piece angle nail plate for trochanteric fractures," *J. Bone Jt. Surg.*, **23**:803-810, 1941.
 - [26] Koch, J.C., "The laws of bone architecture," *Am. J. Anat.*, **21**:177-289, 1917.
 - [27] Kyle, R.F., Wright, J.M. and Burnstein, A.H., "Biomechanical Analysis of the Sliding Characteristics of Compression Hip Screws," *Jr. Bone Jt. Surg.*, **62-A**:1308-1314, 1980.
 - [28] Milch, H., "Photo-elastic studies of bone forms," *Jr. Bone Jt. Surg.*, **22**:621-626, 1940.
 - [29] Mulholland, R.C. and Gunn, D.R., "Sliding screw plate fixation of Inter-trochanteric femoral fractures," *Jr. of Trauma*, **Vol.12 No.7**: 581-591, 1972.
 - [30] Piziali, R.L., Hight, T.K. and Nagel, D. A., "An extended structural analysis of long bones, application to the human tibia," *J. Biomechanics*, **9**:695-701, 1976.
 - [31] Pugh, W.L., "A self-adjusting nail-plate for fractures about the hip-joint," *J. Bone Jt. Surg.*, **37A**:1085-1093, 1955.
 - [32] Pugh, J.W., Rose, R.M. and Radin, E.L., "A structural model for the mechanical behavior of trabecular bone," *J. Biomechanics*, **6**: 657-670, 1973.
 - [33] Roehrle, H., Scholten, R. and Sollbach, W., "Analysis of stress distribution in natural and artificial knee joints on the femur side using Finite Element

Methods," *International Conference Proceedings on Finite Element in Biomechanics*, U. of Arizona Press, Tucson, 781-794, 1980.

- [34] Rohlmann, A., Bergmann, G. and Koelbel, R., "The relevance of stress computation in the femur with and without endoprotheses," *Finite Elements in Biomechanics*(edited by Gallagher, R.H., Simon, B.R., Johnson, P.C. and Gross, J.F.), 361-377, John Wiley, New York, 1982.
- [35] Rybicki, E.F., Simonen, F.A. and Weis, E.B., "On the mathematical analysis of stress in the human femur," *Jr. Biomechanics*, **5**:203- 215, 1972.
- [36] Rybicki, E.F. and Simonen, F.A., "Mechanics of oblique fracture fixation using a Finite Element method," *Jr. Biomechanics*, **10**: 141-148, 1977.
- [37] Rydell, W.W., "Forces acting on the femoral-head prosthesis," *Acta Ortho. Scand.*, **88**:1-132, 1966.
- [38] Simon, B.R., Woo, S.L.Y., Stanley, G.M., Olmstead, S.R., McCarty, M.P., Jemmott, G.F. and Akeson, W.H., "Evaluation of one, two, three dimensional Finite Element and experimental models of internal fixation plates, " *Jr. Biomechanics*, **10**:579-586, 1977.
- [39] Smyth, E.H.J., "The mechanical problem of the artificial hip," *Jr. Bone Jt. Surg*, **43-B**:778-798, 1958.
- [40] Valenta, J., Komarek, P. and Tomcik, J., "Analysis of contact tension in the knee joint," *Acta Chir, Orthop. Trauma. cech*, **48,3**: 257-270, 1981.

- [41] Valliappan, S. Svensson, N.L. and Wood, R.D., "Three-Dimensional Stress analyses of the human femur," *Comput. Bio. Med.*, **7**:253-264, 1977.
- [42] Ward, F.O., "Outlines of human osteology," *H. Renshaw*, London, 1858.
- [43] Williams, J.L. and Lewis, J.L., "Properties and an anisotropic model of cancellous bone from the proximal tibial epiphysis," *J. Biomech. Engg.*, **104**:50-56, 1982.
- [44] Woo, S.L.Y., Simon, B.R., Akeson, W.H. and McCarty, M.P., "An interdisciplinary approach to evaluate the effect of internal fixation plate on long bone, remodeling," *J. Biomechanics*, **10**:87-95, 1977.
- [45] Wood, R. Valliappan, S. and Svensson, N.L., "Stress Analysis of human femur," *Theory and Practice in Finite Element Method Structural Analysis*, Tokyo Seminar (edited by Yamada, Y. and Gallagher, R.H.), 461-478, University of Tokyo Press, Tokyo, 1973.
- [46] Wyman, M.D.J., "Society of natural history," *Boston J. Natural Hist.*, **6**:125-140, 1850-1857.

Comparative Study of Failures in different Plates

TABLE I²²

NO.	TYPE OF NAIL	TYPE OF METAL	ANGLE OF NAIL deg.	AV. MAX. LOAD lbs.	MOUNT. TYPE	TYPE OF FAILURE
1	Thornton plate and Smith-Petersen nail	SMo AISI 316	130	58	3/4" of plate above base	Plate bent
2	Thornton plate and Smith-Petersen nail	SMo S.S.	125	77	3/4" of plate above base	Plate bent
3	Thornton plate and Smith-Petersen nail	316 S.S.	130	58	3/4" of plate above base	Plate bent at top screw hole
4	Thornton plate and Smith-Petersen nail	CoCr alloy No. 1	135	46	3/4" of plate above base	Plate bent at top screw hole
5	McLaughlin	CoCr alloy No. 1	132	133	1 1/8" above mount	Plate bent at top screw hole
6	McLaughlin	316 S.S.	135	103	1 1/8" above mount	Plate bent at top screw hole

7	McLaughlin	SMo S.S.	135	70	1" above mount	Plate bent at top screw plate
8	Temple and Smith-Petersen nail	316 S.S.	135	215	1 1/8" above mount	Smith-Petersen nail bent elastically at load first yield; plate bent at max. load
9	Temple with	316 S.S.	135	357	1/2" above mount	Failure at nail plate junction by stripping of of bolt threads
10	Leinbach	316 S.S.	135	75	3/4" of plate above base	Plate bent at top edge of mount
11	Pugh	SMo S.S.	135	85	1 1/8" of plate above base	Nail telescoped to 3" then plate bent at top screw hole
12	Pugh	SMo S.S.	130	230	1 1/8" of plate above	Nail telescoped to 3" then plate bent at screw hole
13	Massie	316 S.S.	155	186	1/2" of plate above base	Plate bent at edge of mount
14	Neufeld	301 S.S.	130	61	3/4" above mount	Binding at nail plate junction and in upper part of plate

15	Neufeld	CoCr alloy No. 1	130	67	3/4" above mount	Binding at nail junction and in upper part of plate
16	Neufeld	CoCr alloy No. 2	130	42	3/4" above mount	Binding at nail plate junction only
17	V-nail plate	316 S.S.		80	3/4" above mount	Plate bent at edge of mount at top screw hole
18	Jewett old style	SMo S.S.	130	33	Angle 3/4" above mount	Plate bent at edge of mount
19	Jewett- modern	SMo S.S.	130	87	Angle 1 1/8" above mount	Plate bent at edge of mount and at first screw hole
20	Jewett- modern	SMo S.S.	130	169	Angle 1 1/8" above mount	Nail bent elast- ically at load first yield, plate bent at maximum load
21	Jewett- modern	CoCr alloy	130	183	Angle 1" above mount	Plate bent at edge of mount and at top screw hole
22	Jewett- modern	SMo S.S.	130	137	Angle 1 1/8" mount	Plate bent at edge of mount and at top screw hole

23	Jewett-modern #472	316 S.S.	135	311	Angle 1 1/8" above mount	Nail bent first then plate bent
24	Jewett-thin plate	316 S.S.	135	149	Angle 1 1/8" above mount	Plate bent at mount
25	Jewett-cannulated	SMo AISI 316	130	145	Angle 1" above mount	Plate bent at top of mount and at top screw hole
26	Jewett-non-cannulated	SMo AISI 316	130	106	Angle 1" above mount	Plate bent at edge of mount and at top screw hole
27	Key	SMo S.S.	130	241	Angle 1 1/8" above mount	Failure by bending at junction of triffin and round portions of nail and at top screw hole in plate
28	Key	316 S.S.	135	221	Angle 1 1/8" above mount	Plate bent at edge of mount; nail intact.
29	Holt-Austenel	Vitallium	130	300	Angle 7/8" above mount	Four-hole plate bent at top hole
30	Holt-Zimmer(non-cannulated)	Titanium	135	444	Angle 1 1/8" above mount	Four-hole plate broke and fragmented at top screw hole

31	Holt-Zimmer	316 S.S.	135	391	Angle 1 1/8" above mount	Failure by bending maximum at top edge of mount but extended throughout portion of plate above mount
32	Holt-Zimmer(non-cannulated)	A-286	135	769	Angle 1" above mount	Four-hole plate at top screw hole
33	Holt-Austenal	Vitallium	130	845	Angle mounted 3/4 " above edge	Failure by slow bending without fracture first in nail, then in plate

Proportion of Elements in S.S. Nails

TABLE II²²

	301	302	316	317	A-286	Military type MIL-B 16505
C(max.)	0.15	0.15	0.08	0.08	0.08	0.08
Mn(max.)	2.00	2.00	2.00	2.00	1.00-2.00	2.00
P(max.)	0.045	0.045	0.045	0.045	.04	0.03
S(max.)	0.03	0.03	0.03	0.03	0.04	0.03
Si(max.)	1.00	1.00	1.00	1.00	0.04-1.00	0.75
Cr	16.0-18.0	17.0-19.0	16.0-18.0	18.0-20.0	13.5-16.0	17.0-20.0
Ni	6.00-8.00	8.0-10.0	10.0-14.0	11.0-15.0	24.0-28.0	10.0-14.0
Mo			2.0-3.0	3.0-4.0	1.0-1.5	2.0-4.0
Ti					1.50-2.25	
V					0.10-0.50	
Al(max.)					0.35	

Muscle and Joint Forces-Different Walking Cycle

TABLE III⁴⁶

Position during cycle % of cycle after heel strike		1	2	3	4	5
		-2	13	19	50	63
Short flexors-	Total force	0	207	266	276	200
	F _x	0	133	172	173	117
	F _y	0	155	199	213	161
	F _z	0	31	39	26	19
Long flexors-	Total force	0	243	126	0	19
	F _x	0	0	0	0	0
	F _y	0	-243	-126	0	-19
	F _z	0	0	0	0	0
Short - Extensors	Total force	266	0	0	0	0
	F _x	-11	0	0	0	0
	F _y	262	0	0	0	0
	F _z	45	0	0	0	0
Abductors-	Total Force	141	392	460	392	0
	F _x	96	281	334	256	0
	F _y	82	230	283	289	0
	F _z	62	148	141	-68	0
Adductors-	Total Force	0	0	0	0	39
	F _x	0	0	0	0	26
	F _y	0	0	0	0	20
	F _z	0	0	0	0	-21
Ilio-tibial - Tract	Total Force	42	29	34	29	0
	T _x	0	0	0	0	0
	T _y	-42	-29	-34	-29	0
	T _z	0	0	0	0	0
Hip joint - force	Total Force	589	1260	1220	1277	455
	J _x	-429	-552	-562	-488	-140
	J _y	-399	-1110	-1075	-1137	-433
	J _z	61	-225	-130	329	14